Genomic Evidence for Speciation with Gene Flow in Broadcast Spawning Marine Invertebrates

Shotaro Hirase [iD],*,[1] Yo Y. Yamasaki [iD],[2] Masashi Sekino,[3] Masato Nishisako,[4] Minoru Ikeda,[4] Motoyuki Hara,[5] Juha Merilä,[6,7] and Kiyoshi Kikuchi[1]

[1]Fisheries Laboratory, Graduate School of Agricultural and Life Sciences, The University of Tokyo, Maisaka, Hamamatsu, Shizuoka, Japan

[2]Ecological Genetics Laboratory, Department of Genomics and Evolutionary Biology, National Institute of Genetics, Mishima, Shizuoka, Japan

[3]Bioinformatics and Biosciences Division, Fisheries Resources Institute, Japan Fisheries Research and Education Agency, Yokohama, Kanagawa, Japan

[4]Laboratory of Integrative Aquatic Biology, Graduate School of Agricultural Sciences, Tohoku University, Onagawa, Miyagi, Japan

[5]Tohoku Ecosystem-Associated Marine Sciences, Tohoku University, Sendai, Miyagi, Japan

[6]Ecological Genetics Research Unit, Organismal and Evolutionary Biology Research Programme, Faculty of Biological and Environmental Sciences, University of Helsinki, Helsinki, Finland

[7]Research Division of Ecology and Biodiversity, Faculty of Sciences, The University of Hong Kong, Hong Kong SAR, China

*Corresponding author: E-mail: cashirase@g.ecc.u-tokyo.ac.jp.

Associate editor: Keith Crandall

Abstract

How early stages of speciation in free-spawning marine invertebrates proceed is poorly understood. The Western Pacific abalones, *Haliotis discus*, *H. madaka*, and *H. gigantea*, occur in sympatry with shared breeding season and are capable of producing viable F$_1$ hybrids in spite of being ecologically differentiated. Population genomic analyses revealed that although the three species are genetically distinct, there is evidence for historical and ongoing gene flow among these species. Evidence from demographic modeling suggests that reproductive isolation among the three species started to build in allopatry and has proceeded with gene flow, possibly driven by ecological selection. We identified 27 differentiation islands between the closely related *H. discus* and *H. madaka* characterized by high F_{ST} and d_A, but not high d_{XY} values, as well as high genetic diversity in one *H. madaka* population. These genomic signatures suggest differentiation driven by recent ecological divergent selection in presence of gene flow outside of the genomic islands of differentiation. The differentiation islands showed low polymorphism in *H. gigantea*, and both high F_{ST}, d_{XY}, and d_A values between *H. discus* and *H. gigantea*, as well as between *H. madaka* and *H. gigantea*. Collectively, the Western Pacific abalones appear to occupy the early stages speciation continuum, and the differentiation islands associated with ecological divergence among the abalones do not appear to have acted as barrier loci to gene flow in the younger divergences but appear to do so in older divergences.

Key words: marine speciation, ecological speciation, fertilization protein, GRAS-Di, introgression.

Introduction

Long-distance gene flow in the ocean without apparent physical barriers to it is expected to constrain population differentiation and speciation (Palumbi 1992). In particular, speciation in broadcast spawning marine invertebrates is expected to be challenging due to extensive gene flow (Bierne et al. 2003). However, these expectations are contradicted by the high diversity of marine invertebrates in the oceans. Hence, the question how speciation proceeds in the oceans in the absence of geographic isolation remains an important topic in marine biology (Bierne et al. 2003; Palumbi 2009; Puebla 2009).

The process of speciation can be described as a continuum of divergence leading to reproductive isolation, referred to as the "speciation continuum" (Nosil 2012; Seehausen et al. 2014). The later stages of divergence along the speciation continuum are characterized by the evolution of strong barriers to gene flow between species. An example demonstrating such barriers in broadcast spawning marine invertebrates is the coevolution of interacting fertilization proteins, Lysin in sperm and VERL in egg, in the North American abalones (Clark et al. 2009). Many nonsynonymous substitutions among abalone species in the Lysin- and VERL-coding genes have been suggested to prevent interspecies fertilization and cause reproductive isolation in the absence of physical barriers to gene flow. This coevolution was hypothesized to be caused by sexual conflict resulting from polyspermy (Clark et al. 2009); that is, sperm evolves to

Open Access

increase fertilization efficiency, followed by the evolution of eggs to decrease fertilization efficiency, thereby reducing the fertilization of an egg with multiple sperms (i.e., polyspermy) which halts embryonic development. Previous theoretical studies have suggested a model where sexual conflict and ensuing coevolution of interacting fertilization proteins also drive reproductive isolation in the early stages of speciation in broadcast spawning marine invertebrates (Van Doorn et al. 2001). In this model, intraspecific competition for fertilization increases variance in male gamete protein repertoire initiating speciation (Van Doorn et al. 2001). Therefore, interacting fertilization proteins may be responsible for the initial reproductive isolation that eventually led to speciation of the North American abalones.

Ecological factors, such as habitat or temporal isolation, are suggested to be fundamental mechanisms of speciation under situations characterized by the absence of physical barriers to gene flow (Nosil 2012). Barriers to gene flow evolving between populations as a result of ecologically based divergent selection have become known as "ecological speciation" (Nosil 2012). Although this speciation process is expected to be common in the early stages of speciation in marine environments (Lessios 2007; Bester-van der Merwe et al. 2012; Puritz et al. 2012; Rhode et al. 2013; Momigliano et al. 2017), examples of ecological speciation in the ocean are still rare. According to the genomic view of ecological speciation, gene flow is restricted at barrier loci (i.e., loci underlying ecological isolation) clustered in a few genomic regions, but continued in the outside of these regions (speciation with gene flow), leading to the emergence of peaks of genetic differentiation surrounding the barrier loci (i.e., heterogeneous genomic differentiation; Wu 2001; Feder et al. 2012). Also, the speciation with gene flow model must further be distinguished between models where there is no initial period of allopatry or reduced gene flow (i.e., sympatric speciation) and those where gene flow occurs after a substantial period of independent evolution between diverging taxa (i.e., secondary contact; Cruickshank and Hahn 2014). However, empirical genomic data demonstrating such heterogenous differentiation and demographic processes in the early stages of marine speciation are scarce (Palumbi 2009; Pogson 2016; Momigliano et al. 2017). Hence, investigation of genome-wide patterns of genetic differentiation at multiple stages of the speciation continuum in the ocean has been called forth (Puebla 2009; Miglietta et al. 2011).

Here, we focus on the speciation continuum in three species of closely related Western Pacific abalones: *Haliotis discus*, *H. madaka*, and *H. gigantea* (fig. 1A; Ino 1952). Of these, *H. discus* is distributed widely along the coasts of the Japanese archipelago and the Korean Peninsula, and it is classified into two subspecies due to slight morphological differences in dorsal surface of the shell (Ino 1952). *Haliotis discus hannai* is distributed throughout northern Japanese and Korean coasts, whereas *H. discus discus* has more southern distribution along Japanese and Korean coasts (Ino 1952; Hara and Sekino 2005; Nam et al. 2021; fig. 1A). However, their geographic distribution ranges have not been accurately determined in Japan (fig. 1A). On the other hand, *H. madaka* and *H. gigantea* tend to be endemic to the Japanese archipelago and occur in sympatry with the subspecies *H. discus discus* in the southern Japanese coast (fig. 1A) sharing the same breeding season (Ino 1952). Previous genetic studies using allozyme (Hara and Fujio 1992), mitochondrial DNA (An et al. 2005), microsatellite DNA (Sekino and Hara 2007a), and the *Lysin* gene (Lee and Vacquier 1995) variability have shown that the three species are closely related but differ in the degree of
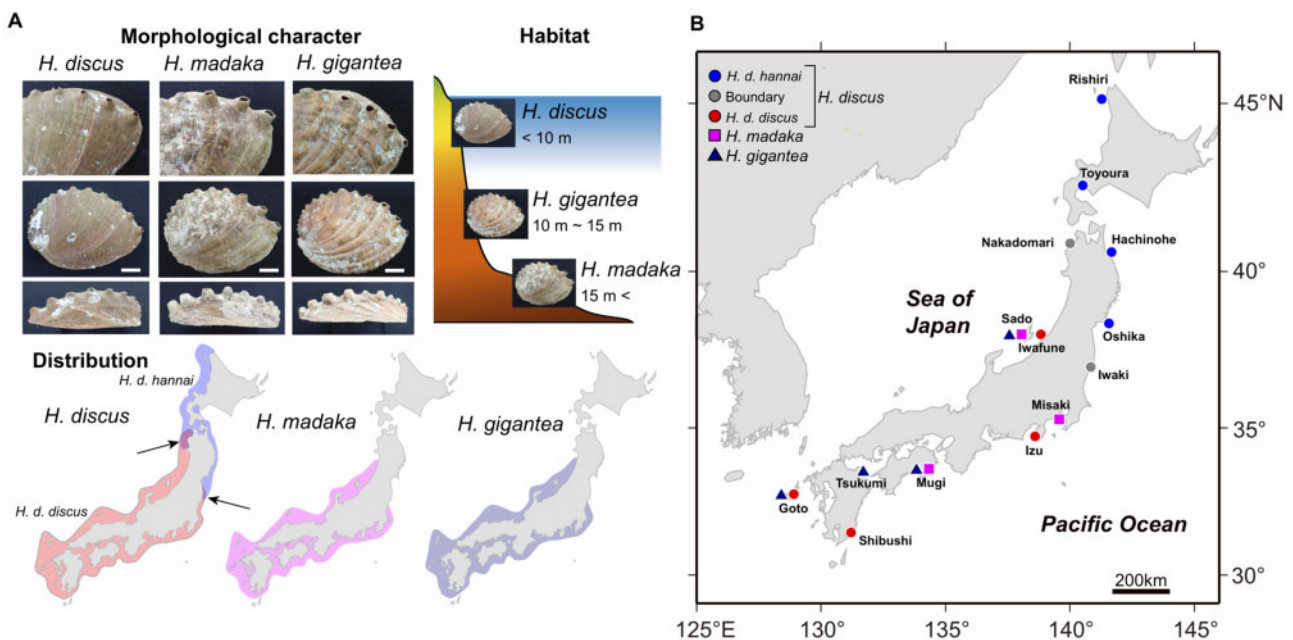

FIG. 1. (A) Morphological and ecological features, as well as geographical distributions of the Western Pacific abalones in Japan. The scale bars in the (A) corresponds to 2 cm. Arrows in the distribution map of *Haliotis discus* show boundary zones between the two subspecies, *H. discus hannai* and *H. discus discus*. (B) Sampling locations of the Western Pacific abalones used in this study.

divergence from each other; *H. gigantea* is genetically distinct from *H. discus* and *H. madaka*. The three species are also morphologically distinct and occupy different depth zones (fig. 1A; Ino 1952; Itami et al. 1978; Sakai and Shimamoto 1978), but can produce viable F_1, F_2, and backcross generation offspring in experimental settings (Koike et al. 1988; Ahmed et al. 2008), suggesting that prezygotic and postzygotic isolation is still incomplete. Hence, it appears that the Western Pacific abalones in the Japanese archipelago may be in the early stages of speciation triggered by ecological factors such as the differences in habitat selection, providing an opportunity to investigate the evolutionary processes and genomic architecture along the speciation continuum in broadcast spawning marine invertebrates.

To address how far speciation has proceeded along the speciation continuum, we examined the patterns of genomic divergence in the Western Pacific abalones using nuclear single nucleotide polymorphism (SNP) loci obtained with a cost-effective nontargeting polymerase chain reaction (PCR)-based sequencing method, genotyping by random amplicon sequencing, direct (GRAS-Di; Enoki and Takeuchi 2018; Hosoya et al. 2019) and whole-genome sequencing, as well as with mitochondrial genome sequencing. Based on these genomic data, we examined the patterns and degree of genomic divergence among the three abalone species, with focus on identifying genomic regions showing evidence for divergent selection. We also performed demographic modeling to infer divergence times and patterns of gene flow among the three species based on analyses of the site-frequency spectrum (SFS).

Results

Close Phylogenetic Relationships among the Western Pacific Abalones

The RAxML tree (Stamatakis 2014) based on 46,366 SNP loci common to the North American and the Western Pacific abalones derived from whole-genome sequencing data suggested that the genetic distances among the Western Pacific abalones are very small in comparison to those among six North American abalones (fig. 2A). This result suggests that speciation of the Western Pacific abalones has occurred more recently than that of the North American abalones which are thought to be reproductively isolated (Clark et al. 2009). Similarly, the RAxML tree of the Western Pacific abalones based on 18,109 SNP loci derived from GRAS-Di demonstrated small but clear genetic differentiation among *H. discus*, *H. madaka*, and *H. gigantea* (fig. 2B). Given that the three species are caught in sympatry by local fishermen in our study sites (fig. 1B), the result suggests that the species are undoubtedly reproductively isolated.

However, the phylogenetic tree based on mitochondrial genome data was not consistent with the phylogenetic tree based on nuclear genomic data; whereas all *H. gigantea* individuals fell into one of the four clades, the other three clades were shared among *H. discus*, and *H. madaka* populations (fig. 2C). Moreover, analysis of molecular variance (AMOVA) based on mitochondrial genome data did not show genetic differentiation between *H. discus* and *H. madaka* (AMOVA, $P > 0.05$). These results may be attributed to the recent establishment of reproductive isolation between *H. discus* and *H. madaka* and/or ongoing hybridization between these species. Two mitochondrial haplotypes detected in two *H. madaka* individuals were close to the *H. gigantea* clade and located at basal positions (fig. 2C), suggesting that this haplotype sharing is not attributable to recent hybridization.

Coevolution of *Lysin-* and *VERL-* Genes Is Not Associated with Reproductive Isolation

Interspecies nonsynonymous substitutions in the *Lysin* and *VERL* genes are involved in the reproductive isolation among the North American abalones (Clark et al. 2009). Therefore, interspecies nonsynonymous substitutions in the two genes may be also associated with reproductive isolation among the Western Pacific abalones. However, such nonsynonymous substitutions within the Western Pacific abalones have been reported only in the *Lysin* gene of *H. gigantea* (Lee and Vacquier 1995); intraspecific polymorphisms in *Lysin* genes of the Western Pacific abalones and substitutions in *VERL* genes of the Western Pacific abalones have not been investigated yet. Our gene annotation suggested that both of *Lysin* (HDSC01187: 6,572–33,666) and *VERL* (HDSC09152: 4,839–9,463) genes were included in the *H. discus hannai* reference genome (Nam et al. 2017). Hence, we next examined whether nonsynonymous substitutions occur in the *Lysin* and *VERL* genes of *H. madaka* and *H. gigantea* against the *H. discus hannai* reference genome (Nam et al. 2017) using whole-genome sequencing data.

Consistent with the results of the previous study (Lee and Vacquier 1995), there were one synonymous and four nonsynonymous substitutions in the first exon of the *Lysin* gene, for which positive selection was suggested (Clark et al. 2009), in *H. gigantea* (supplementary table 1, Supplementary Material online). In contrast, we found no nonsynonymous substitution between *H. discus* and *H. madaka* in the *Lysin* gene (supplementary table 1, Supplementary Material online). In all species, intraspecific polymorphism was absent, suggesting selective sweep in this gene as suggested in the North American abalones (Clark et al. 2009). VERL comprised 22 protein repeats, and the first two repeats (repeat 1 and 2) are the most different from other repeats. Among these repeats, VERL repeat 2 is considered to play a role in species-specific sperm selection (Galindo et al. 2003). However, we found nonsynonymous substitution in the coding region of VERL repeats 1 and 2 neither in *H. madaka* nor in *H. gigantea*, suggesting that the coevolution of *Lysin* and *VERL* genes has not occurred in all Western Pacific abalones. Therefore, this finding raises the possibility that some other factors rather than the coevolution of fertilization proteins, such as ecological factor(s), contribute to reproductive isolation in the Western Pacific abalones.

Footprints of Recent and Historical Hybridization

Given the close phylogenetic relationships and shared mitogenome haplotypes among *H. discus*, *H. madaka*, and *H. gigantea* (figs. 2A–C), hybridization may have occurred
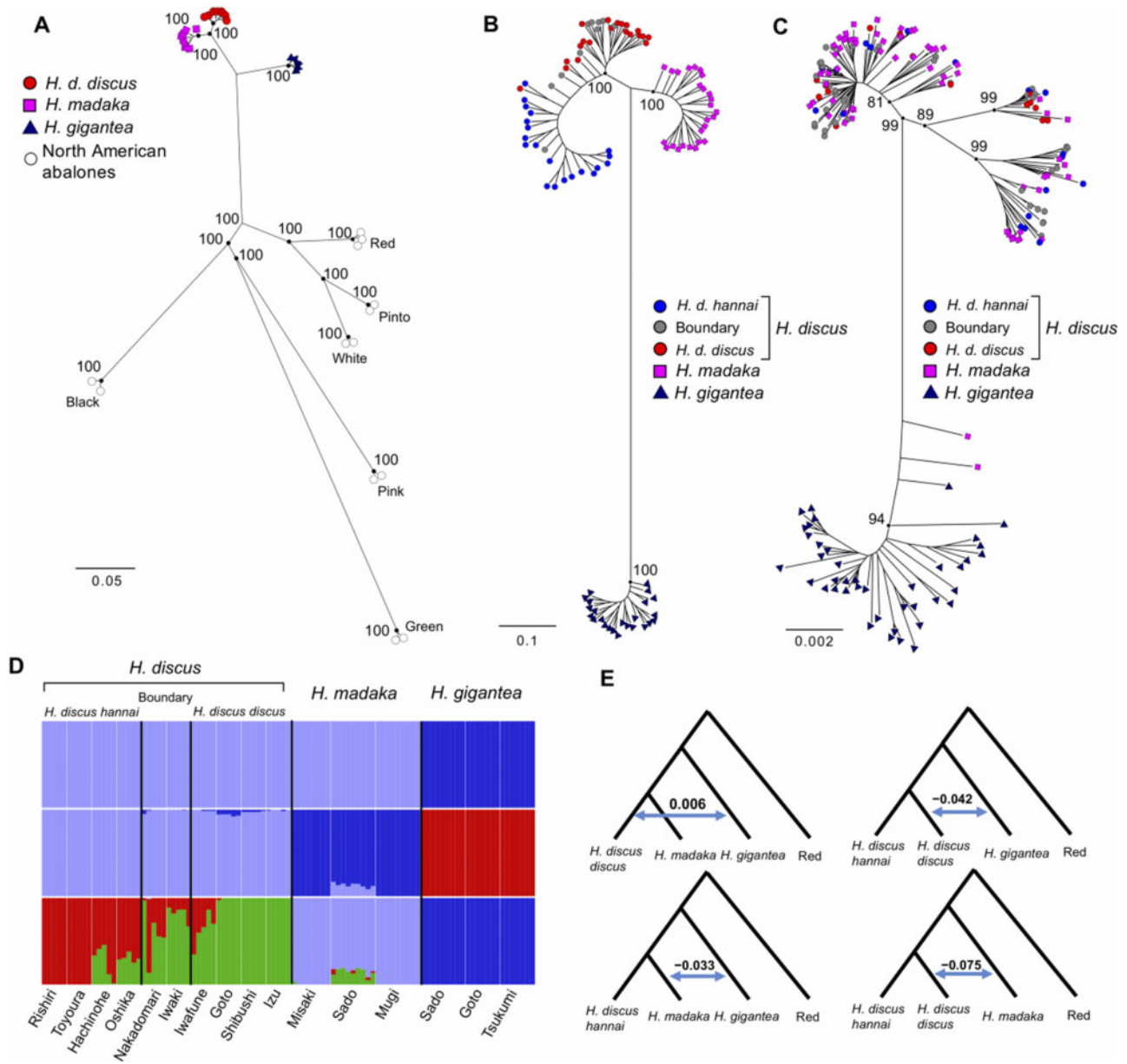
Fig. 2. (A) ML tree of the Western Pacific and the North American abalones (Red: *Haliotis rufescens*, Pinto: *H. kamtschatkana*, White: *H. sorenseni*. Black: *H. cracherodii*, Pink: *H. corrugate*, Green: *H. fulgens*) based on whole-genome sequencing data (46,366 SNP loci). (B) ML tree of the Western Pacific abalones based on GRAS-Di data (18,109 SNP loci). (C) Neighbor-joining tree based on the mitochondrial genomes of the Western Pacific abalones. The values in the nodes in (A)–(C) are bootstrap values. (D) Individual admixture proportions (*q*-values) among the Western Pacific abalones estimated by ADMIXTURE. (E) D-statistics of the Western Pacific abalones (z-score [D-statistic/standard error] > 3). The Red abalone (*H. rufescens*) was used as an outgroup in calculation of D-statistics.

among the three abalone species. To get insight into this possibility, we set to evaluate the degree of gene flow among the three abalone species. In clustering analyses using ADMIXTURE (Alexander et al. 2009) with GRAS-Di data, the cross-validation error reached a plateau at around $K = 4$ (supplementary fig. 1, Supplementary Material online). When assuming $K = 4$, *H. discus* was assigned into two genetic clusters corresponding to *H. discus hannai* and *H. discus discus*, and these two genetic clusters admixed in putative boundary zones (fig. 2D). *Haliotis madaka* and *H.*

gigantea were also assigned into different genetic clusters (fig. 2D), suggesting limited gene flow among three abalone species.

However, the *H. madaka* population in Sado showed clear signatures of genomic introgression from *H. discus discus* in the ADMIXTURE plot (fig. 2D). For each of the putative hybrid individuals of *H. madaka* population in Sado, we genotyped 76 SNP loci in 46 scaffolds (parts of these SNP loci are located closely to each other in same scaffold) that were fixed for different alleles in each of *H. discus* and *H. madaka*.

Consistent with the ADMIXTURE results, the genotype data based on the 76 SNP loci showed clear signatures of allele sharing between *H. discus* and the Sado population of *H. madaka* (supplementary fig. 2, Supplementary Material online). One can expect that first-generation (F_1) hybrids would be consistently heterozygous at nearly all of the 76 SNP loci. However, because all of the putative hybrids failed to conform to this expectation, they could be second-generation (F_2) hybrids, backcrosses, or later-generation hybrids. NewHybrids analysis (Anderson and Thompson 2002) based on 76 SNP loci assigned four putative hybrids to be backcrosses to *H. madaka*, and five putative hybrids to be pure *H. madaka* with 100% posterior probability (supplementary table 2, Supplementary Material online). Given that *H. discus discus* and *H. madaka* are co-distributed in Sado, it can be inferred that *H. discus discus* and pure (or nearly pure) *H. madaka* have hybridized and even backcrossed to *H. madaka* there recently. It is notable that number of inter-scaffold SNP pairs showed high r^2 values (>0.5). This suggests that they are either in close physical proximity of each other, or strong positive selection due to possible functional associations maintains this high linkage disequilibrium (LD) (supplementary table 3, Supplementary Material online). Although ADMIXTURE analyses did not find any evidence of hybridization except in *H. madaka* in Sado, ABBA–BABA analyses based on whole-genome sequencing data showed signals of hybridization among *H. discus discus*, *H. madaka*, and *H. gigantea*, which overlap in their geographic distributions (z-score [D-statistic/standard error] > 3; fig. 2E). Altogether, these findings suggest that the strength of reproductive isolation between *H. discus* and *H. madaka* varies regionally and that the Western Pacific abalones have hybridized historically.

Demographic Modeling Supported Speciation-with-Gene Flow Model

The aforementioned genomic analyses implied that the Western Pacific abalones have speciated in the face of gene flow. To test this hypothesis, we performed demographic modeling based on the SFS using fastsimcoal2 (Excoffier et al. 2013). In this analysis, we used GRAS-Di data from sympatric *H. discus discus*, *H. madaka* (except for the Sado population with recent hybridization), and *H. gigantea* populations. First, we compared nine demographic models (fig. 3A); one model assumed no gene flow during the speciation process (Model 1), whereas the other eight models (Models 2, 3, 4, 5, 6, 7, 8, and 9) assumed gene flow in different pairs of species or an ancestor. To simplify the models, we assumed constant population size for each species. The highest log-likelihood and lowest Akaike information criterion (AIC) were obtained for Model 9 (fig. 3A and C). Model 9 assumed speciation with gene flow for both the initial divergence of *H. gigantea* and subsequent divergence between *H. discus discus* and *H. madaka*, and gene flow between *H. discus discus* and *H. gigantea*, and between *H. madaka* and *H. gigantea*, which is consistent with the result of ABBA–BABA analyses (fig. 2E).

For speciation with gene flow model, we must further distinguish between models where there is no initial period of allopatry or reduced gene flow (i.e., sympatric speciation) and those where gene flow occurs after a substantial period of independent evolution between diverging taxa (i.e., secondary contact; Cruickshank and Hahn 2014). Hence, we compared the Model 9 with its derivate model that assumes allopatric phase or reduced gene flow in the divergence event between *H. discus discus* and *H. madaka* (Model 10), and higher log-likelihood and lower AIC were obtained for Model 10 (fig. 3B and C). Next, we compared Model 10 with its derivate model that assumes allopatric phase or reduced gene flow between *H. gigantea* and an ancestor of *H. discus discus* and *H. madaka* (Model 11), and the higher log-likelihood and lower AIC were obtained for Model 11 assuming secondary contact between *H. gigantea* and an ancestor of *H. discus discus* and *H. madaka* (fig. 3B and C). Consequently, demographic modeling suggested that both speciation events in the Western Pacific abalones started with allopatric or reduced gene flow phase followed by secondary contact.

The parameter estimates based on Model 11 show an interesting pattern of gene flow; the rate of gene flow from *H. discus discus* to *H. madaka* was higher than that from *H. madaka* to *H. discus discus* (fig. 3D). This pattern is consistent with the results of the clustering analyses using ADMIXTURE, which suggested genomic introgression from *H. discus discus* to *H. madaka* abalones in Sado (fig. 2D). Although the *H. madaka* population in Sado was not included in this demographic modeling, this suggests that directional genomic introgression may have occurred there too.

Potential Genomic Regions Resistant to Gene Flow

Given the close relationship (median $F_{ST} = 0.007$; fig. 4) as well as historical and ongoing hybridization between *H. discus* and *H. madaka*, highly divergent genomic regions between *H. discus* and *H. madaka* are candidate targets of divergent selection, that is, "barrier loci" (Feder et al. 2012). The above mentioned 76 SNP loci that were fixed for different alleles in *H. discus* and *H. madaka* (except for Sado population) are such candidates (fig. 4). To identify such genomic regions further, we performed SNP-based genome scans based on GRAS-Di data using *pcadapt* (Luu et al. 2017), Fdist (Beaumont and Nichols 1996), BayeScan (Foll and Gaggiotti 2008), and FLK (Bonhomme et al. 2010) using all *H. discus* and *H. madaka* individuals. As a result, we found 148 outlier SNP loci (16 fixed SNP loci were also included) that were detected by all four methods (fig. 4). Similarly to loci fixed to different alleles between *H. discus* and *H. madaka*, some of these outlier SNP loci also showed high inter-scaffold r^2 values (>0.5) in *H. madaka* in Sado (supplementary table 4, Supplementary Material online).

We next investigated whether the 76 fixed and the 148 outlier SNP loci were located in divergent genomic regions identified with the aid of 5.9 million SNP loci obtained from the whole-genome sequencing data. We did this by searching divergent genomic regions (in 20-kb windows) showing up in the top 1% of the F_{ST} distribution between *H. discus* and *H. madaka*. This search yielded 23 fixed and 30 outlier SNP loci overlapping divergent genomic regions in 27 different scaffolds (fig. 5A; table 1; henceforth referred to as "23 divergent
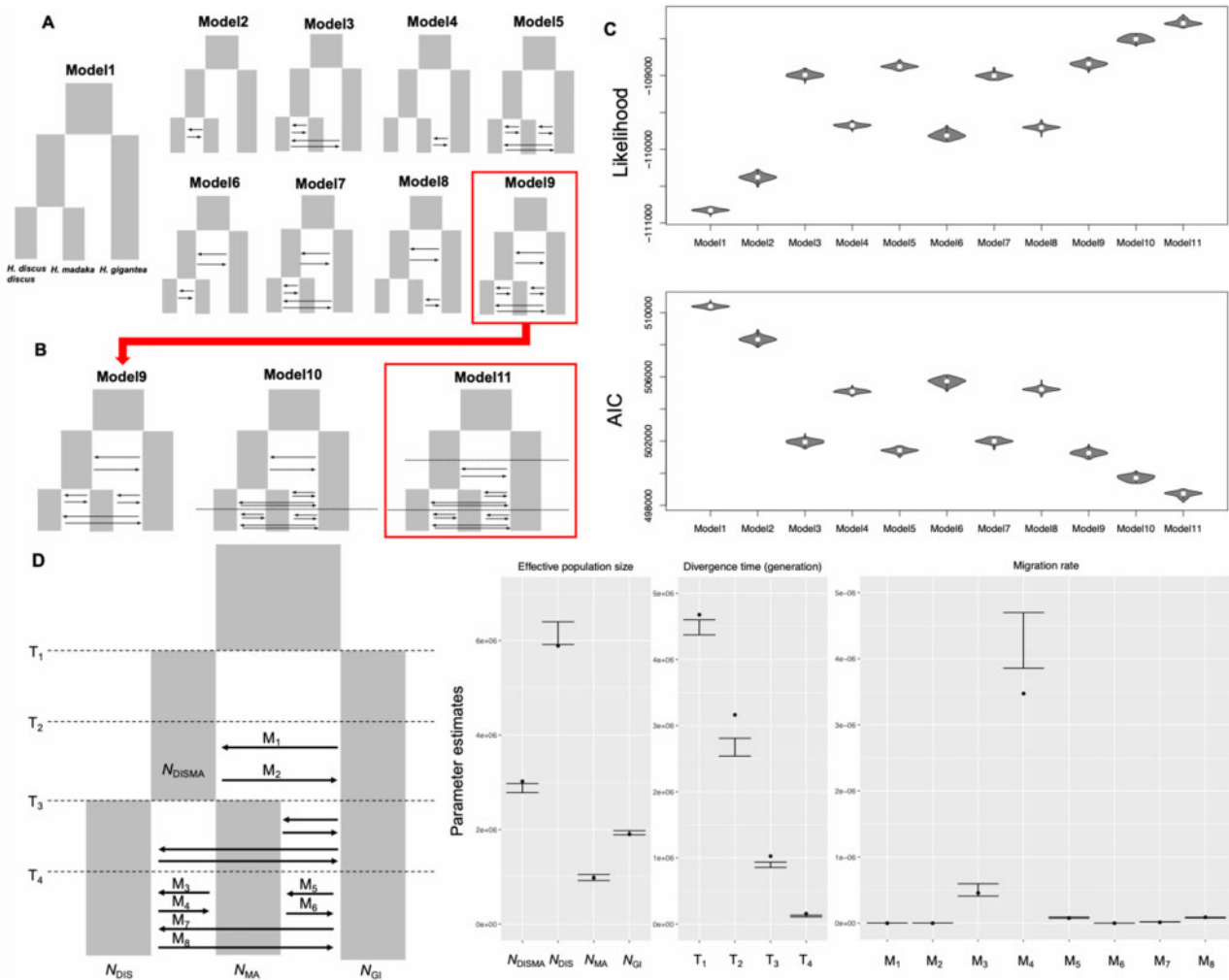
FIG. 3. SFS-based coalescent analyses for modeling Western Pacific abalone speciation. (A) Nine demographic models tested. (B) Three demographic models with and without secondary contact based on Model 9 that supported by first-round demographic modeling. (C) Distributions of $\log_{10}$ likelihood and AIC from 100 expected SFS each approximated using 1 million coalescent simulations under the parameters that maximize the likelihood for each model. (D) Parameter estimates of effective population sizes, the times of divergences, migration rates, and their associated 95% CIs derived from nonparametric block bootstraps. N_{DISMA}, effective population size (N_e) of a common ancestor of *Haliotis discus* and *H. madaka*; N_{DIS}, N_e of *H. discus*; N_{MA}, N_e of *H. madaka*; N_{GI}, N_e of *H. gigantea*; T_1 and T_2, times of divergences (in generations); M_1–M_8, migration rates.

SNP loci," "30 selected outliers," and "27 differentiation islands" [Burri 2017]). The number of these overlaps were confirmed to be significantly higher than expected on the basis of random sampling of SNP loci (max. 6 overlapping loci for 148 SNP loci and max. 4 overlapping loci for 76 SNP loci; $P < 0.001$). Observed heterozygosity in the 30 selected outliers, as well as that in the 23 divergent SNP loci, was lower than that of other loci in all populations with the exception of *H. madaka* population in Sado where genomic introgression from *H. discus* was detected (fig. 5B). Nucleotide diversity (*pi*) in 27 differentiation islands was also lower than other genomic regions in all abalones, suggesting that these islands are under divergent selection (fig. 5C).

If the 27 differentiation islands have been involved in reducing gene flow between sympatric *H. discus* and *H. madaka* since the early stages of divergence, they are expected to show both high F_{ST} and high absolute sequence divergence (d_{XY}:

Nei and Li 1979) as pointed out by Cruickshank and Hahn (2014). This is because divergence is expected to be initiated in the regions with reduced gene flow, resulting in both high F_{ST} and elevated nucleotide divergence. To test this, we estimated d_{XY} for the 27 differentiation islands. Unexpectedly, the values of d_{XY} of the identified differentiation islands were not significantly higher than the genomic background (Wilcoxon rank-sum test; $P > 0.05$; fig. 5D; table 1). On the other hand, 4 of the 27 differentiation islands (scaffolds HDSC00375, HDSC01503, HDSC01562, and HDSC04393) had d_{XY} values above the 90th percentile of the genome-wide distribution (table 1). Because introgression from *H. gigantea* to either *H. discus* or *H. madaka* can also elevate both F_{ST} and d_{XY} (Jones et al. 2018; Oziolor et al. 2019), the possibility of introgression in 27 differentiation islands was evaluated based on sliding-window-based f_d-statistics, a modified version of ABBA–BABA statistics (Martin et al. 2015). Of
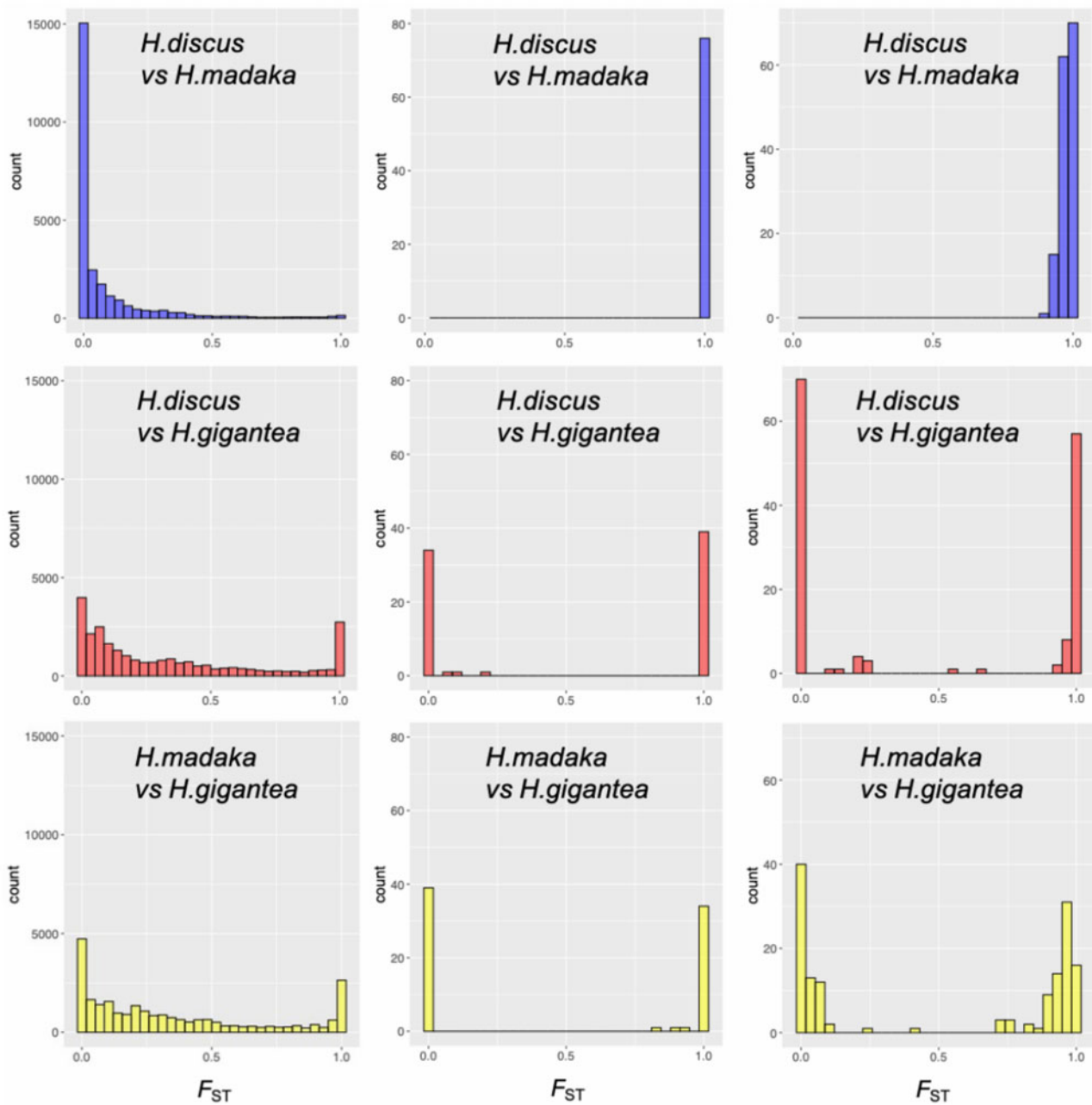
Fig. 4. Histograms of site-F_{ST} values of all SNPs (left), 76 fixed SNPs (middle), and 148 common outlier SNPs (right).

the four differentiation islands with both high F_{ST} and high d_{XY}, differentiation islands within the HDSC01562 and HDSC04393 scaffolds showed high f_d values above 90th percentile, suggesting that they might originate from introgression (table 1). Consequently, only two of the differentiation islands (in scaffolds HDSC00375 and HDSC01503) exhibited features of high F_{ST} and high d_{XY} expected from barrier loci allowing speciation with gene flow.

Although d_{XY} between *H. discus* and *H. madaka* in the 27 differentiation islands was not high, the values of d_A (Nei and Li 1979) were significantly higher than the genomic background (Wilcoxon rank-sum test; $P < 0.05$; fig. 5E; table 1). d_A value is obtained by subtracting *pi* of the two lineages from d_{XY}, and this measure captures pairwise differences that arose

since the lineage split (Burri 2017). Therefore, the high d_A value suggests that although nucleotide divergence between *H. madaka* and *H. discus* due to divergent selection has certainly been accumulating in the differentiation islands, relatively high within-species *pi* have elevated absolute d_{XY} in their genomic backgrounds (fig. 5C) and lead to the low d_{XY} in the differentiation islands.

Several previous studies demonstrate that high F_{ST} is seldom associated with high d_{XY} (Cruickshank and Hahn 2014). Such pattern of differentiation can be caused by recurrent background selection before and after speciation, but not by reduced gene flow (Begun et al. 2007; Cruickshank and Hahn 2014; Burri 2017; Ravinet et al. 2017). If background selection has contributed to high F_{ST} and unaffected d_{XY} in
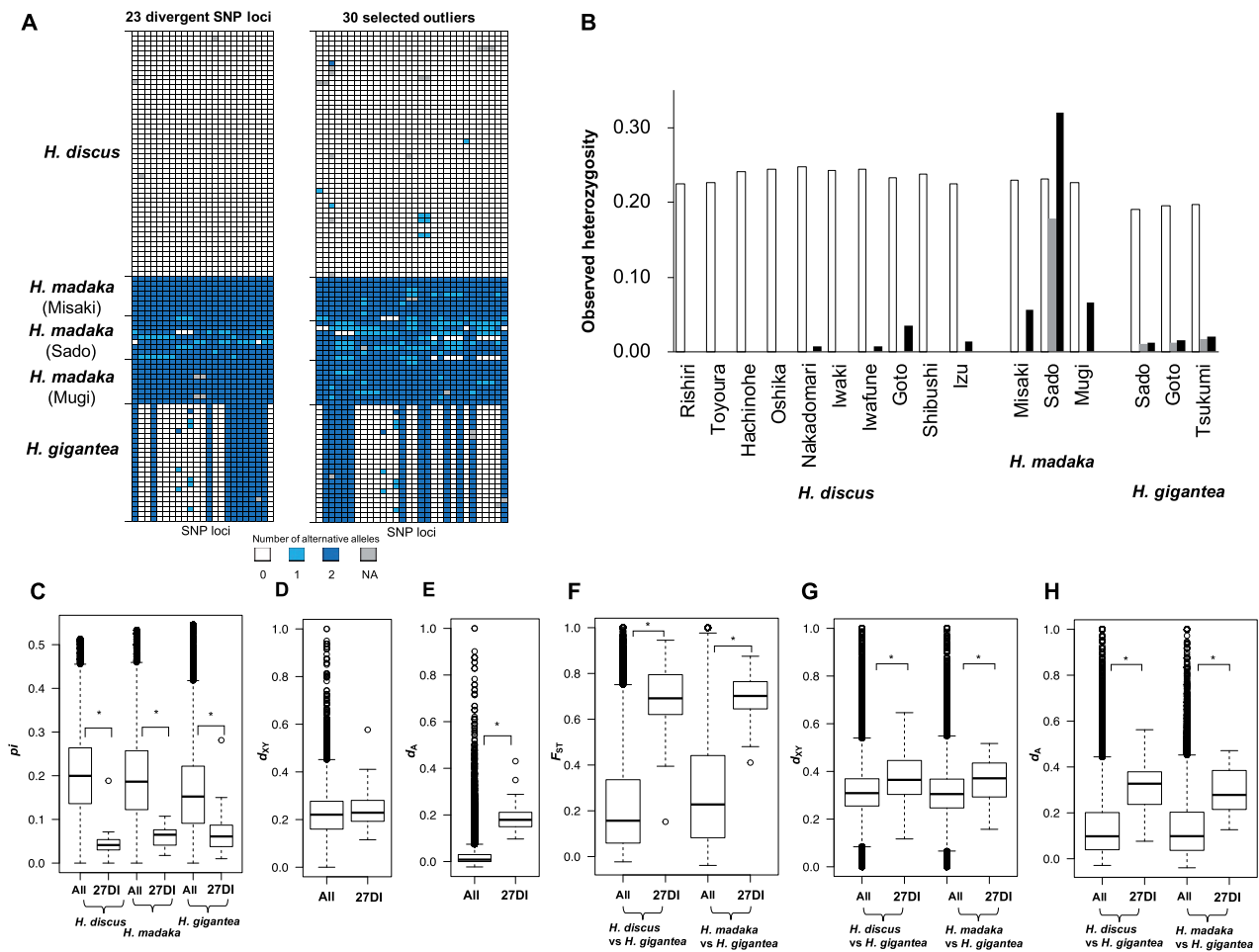
FIG. 5. (A) Genotypes in 23 divergent and 30 selected outlier SNP loci showing the genetic divergence between *Haliotis discus* and *H. madaka* abalones. NA shows loci that were not gentyped. (B) Observed heterozygosity in each of the three Western Pacific abalone populations across all SNP loci (white), 23 divergent SNP loci (gray), and 30 selected outlier (black). (C) Boxplot of nucleotide diversity (*p*i) in *H. discus*, *H. madaka*, and *H. gigantea* in all and 27 differentiation islands (27DI). (D) Boxplot of absolute sequence divergence (d_{XY}) between *H. discus* and *H. madaka* in all and 27DI. (E) Boxplot of net sequence divergence (d_A) between *H. discus* and *H. madaka* in all and 27DI. (F) Boxplot of sliding-window F_{ST} values between *H. discus* and *H. gigantea*, and between *H. discus* and *H. gigantea* in all and 27DI. (G) Boxplot of d_{XY} between *H. discus* and *H. gigantea*, and between *H. discus* and *H. gigantea* in all and 27DI. (H) Boxplot of d_A between *H. discus* and *H. gigantea*, and between *H. discus* and *H. gigantea* in all and 27DI. Asterisks show significant differences (Wilcoxon rank-sum test; $P < 0.05$).

differentiation islands, comparisons between *H. discus* and *H. gigantea*, and between *H. madaka* and *H. gigantea* should also show high F_{ST} and unaffected d_{XY} because background selection is not expected to be a lineage-specific (Burri 2017). However, contrary to this expectation, these F_{ST} and d_{XY} values exceeded significantly the genomic background levels as well as d_A values (Wilcoxon rank-sum test; $P < 0.05$; fig. 5F–H; table 1). In addition, *p*i in each of 27 differentiation islands was low in not all species (table 1). These results suggest that background selection cannot explain unaffected d_{XY} between *H. discus* and *H. madaka* and that most of the differentiation islands have reduced gene flow between *H. gigantea* and *H. discus* or *H. madaka*, with older divergences. On the other hand, one differentiation island (in scaffold HDSC04994) showed low *p*i in all three species and unaffected d_{XY} in all species pairs, and thus, this island may have been generated by background selection. In addition to background selection, local adaptation following or unrelated to speciation has also

been suggested to result in high F_{ST} and unaffected d_{XY} values (Cruickshank and Hahn 2014; Ravinet et al. 2017). However, given high F_{ST} and high d_{XY} between *H. discus* and *H. gigantea*, and between *H. madaka* and *H. gigantea*, it is unlikely that the 27 differentiation islands are involved in local adaptation of *H. madaka* and *H. discus*.

The 27 differentiation islands included 13 annotated genes (table 1). Among these genes, the 26S proteasome non-ATPase regulatory subunit 10 (*PSMD10*) that was included in the differentiation island of HDSC 06434 has been reported to change oxidative stress-related pathways in the muscle of the white leg shrimp *Litopenaeus vannamei* in response to increased salinity (Wang et al. 2015). Also, the Ankyrin gene, the motif of which is included in *PSMD10*, is a candidate gene of local adaptation in Red abalone (De Wit and Palumbi 2013). Therefore, this gene might be related to the adaptive differentiation also in Western Pacific abalones. Indeed, SnpEff (Cingolani et al. 2012) analyses revealed the presence of

Table 1. Twenty-Seven Divergent Genomic Regions between Closely Related *Haliotis discus* and *H. madaka*.

Scaffold	Divergent Loci	Selected Outliers	top 1% F_{ST} Window (HD vs. HM)	d_{XY} (HD vs. HM)	d_A (HD vs. HM)	f_d (HD–HG)	f_d (HM–HG)	π (HD)	π (HM)	π (HG)	F_{ST} (HD vs. HG)	F_{ST} (HM vs. HG)	d_{XY} (HD vs. HG)	d_{XY} (HM vs. HG)	d_A (HD vs. HG)	d_A (HM vs. HG)	Linkage group	Annotated gene
HDSC0060	639957	639786, 639957	620,001–640,000	0.169	0.138*		0.011	0.0295†	0.0312†	0.0786	0.793*	0.810*	0.487*	0.487*	0.433*	0.432*	LG17	
HDSC0194	596133		580,001–600,000	0.273	0.299**		0.134	0.0712†	0.0707	0.0323†	0.635*	0.694*	0.351	0.294	0.299	0.243	LG16	SSTR2
HDSC0283	87998, 88035		80,001–100,000	0.235	0.454**	0.027		0.0274†	0.0655†	0.0506	0.834*	0.766*	0.493*	0.439	0.454*	0.381*	LG01	SPR
HDSC0375		244254	240,001–260,000	0.336*	0.265**		0.130	0.0709†	0.0701	0.0869	0.632*	0.628*	0.432	0.336	0.353*	0.257		
HDSC0833	448991, 448996, 449000		440,001–460,000	0.246	0.192*		0.041	0.0115†	0.0613†	0.0390†	0.796*	0.640*	0.218	0.231	0.192	0.181	LG07	NCL
HDSC0857		128388, 128389, 128528	120,001–140,000	0.208	0.163*	0.004		0.0355†	0.0551†	0.0610	0.693*	0.650*	0.306	0.269	0.258	0.211		CNOT11
HDSC0971		73261, 73267, 73295, 73302	60,001–80,000	0.288	0.213**		0.279*	0.0686†	0.0818	0.0100†	0.567*	0.717*	0.238	0.300	0.199	0.254	LG13	
HDSC1372		307426	300,001–320,000	0.251	0.134*		0.035	0.0413†	0.0552†	0.0512	0.687*	0.699*	0.311	0.298	0.334**	0.337*	LG01	GATA3
HDSC1400	162134, 162148, 162000	162134, 162148, 162185	160,001–180,000	0.180	0.203**	0.014	0.298*	0.0500†	0.0410†	0.0696	0.689*	0.763*	0.394	0.392	0.265	0.244		SLC6A14
HDSC1500		127929	120,001–140,000	0.300	0.251**	0.045		0.0390†	0.0586†	0.1017	0.610*	0.580	0.301	0.290	0.231	0.209	LG11	
HDSC1503	62447, 62466		60,001–80,000	0.348*	0.288**		0.107	0.0509†	0.0686†	0.2813	0.395	0.411	0.354	0.394	0.187	0.219		
HDSC1562	42647, 42668		40,001–60,000	0.411*	0.350**		0.298*	0.0575†	0.0649†	0.1066	0.529*	0.558	0.295	0.292	0.213	0.206		
HDSC1641	284248, 284249		280,001–300,000	0.115	0.342**	0.009		0.0195†	0.0175†	0.0249†	0.857**	0.872**	0.365	0.299	0.342*	0.278	LG04	BECN1
HDSC2293		286533	280,001–300,000	0.229	0.179*	0.006		0.0713†	0.0283†	0.0303†	0.657*	0.875**	0.378	0.432	0.327*	0.403*		
HDSC2343	93665		80,001–100,000	0.151	0.349**	0.019		0.0314†	0.0437†	0.0307†	0.802*	0.817*	0.380	0.371	0.349*	0.334*		
HDSC2435	46386		40,001–60,000	0.222	0.405**		0.037	0.0457†	0.0701	0.0644	0.746*	0.745*	0.460*	0.457*	0.405*	0.390*		
HDSC2598		98883, 98953, 98963	80,001–100,000	0.231	0.166*		0.062	0.0473†	0.0826	0.0901	0.676*	0.663*	0.399	0.419	0.330*	0.332*		
HDSC3044	88188		80,001–100,000	0.224	0.477**	0.023		0.0308†	0.0300†	0.0619	0.820*	0.846*	0.524*	0.517*	0.477*	0.471*		
HDSC3119	57856		40,001–60,000	0.163	0.336**			0.0518†	0.0264†	0.0558	0.698*	0.828*	0.390	0.412	0.336*	0.370*		
HDSC3434	5718		1–20,000	0.240	0.276**	0.035		0.0366†	0.0846	0.0710	0.691*	0.480	0.329	0.221	0.276	0.143		
HDSC3507		14619	1–20,000	0.202	0.157*		0.029	0.0558†	0.0341†	0.1123	0.747*	0.745*	0.646*	0.462*	0.562*	0.389*		
HDSC3534	35699		20,001–40,000	0.183	0.250**		0.017	0.0087†	0.0701	0.0365†	0.857**	0.655*	0.272	0.261	0.250	0.208		SCRN3
HDSC4345		116238	100,001–120,000	0.218	0.159*		0.037	0.0321†	0.0857	0.0869	0.771*	0.704*	0.476*	0.491*	0.416*	0.404*		
HDSC4393		10800, 11024, 11028	1–20,000	0.580**	0.431**	0.682**		0.1880	0.1043	0.0395†	0.152	0.702*	0.190	0.427	0.076	0.355*	LG02	DPEP1
HDSC4994		205736	200,001–220,000	0.152	0.119*	n.e	0.022	0.0247†	0.0412†	0.0202†	0.590*	0.666*	0.117	0.157	0.094	0.127	LG11	DHODH, ZNF121
HDSC6394	27870, 27872		20,001–40,000	0.225	0.242**	0.006		0.0437†	0.0959	0.1501	0.563*	0.489	0.340	0.347	0.243	0.224		CFAP221
HDSC6434	33688, 33720, 33772	33688	20,001–40,000	0.289	0.235**		n.e	0.0000†	0.1073	0.0417†	0.945*	0.733*	0.479*	0.503*	0.458*	0.428*		PSMD10

Note.—HD, *Haliotis discus*; HM, *Haliotis madaka*; HG, *Haliotis gigantea*; π, nucleotide diversity; d_{XY}, absolute sequence divergence; d_A, net sequence divergence. The f_d value of HDSC06434 was not estimated due to low nucleotide diversity. **Above 99 percentile; *above 90 percentile; †below 10 percentile.

divergent nonsynonymous substitutions among the three abalones in *PSMD10* genes. Each species has different combinations of these substitutions, that is, haplotypes, which may be associated with the expression of different phenotypes among the three abalone species (supplementary fig. 3, Supplementary Material online). Other genomic regions also include functionally interesting genes (table 1). For example, the sex peptide receptor (*SPR*) that included in the differentiation island of HDSC00375 scaffold has been studied in the fruit fly *D. melanogaster*, and it has an important function in determining reproductive behavior (Yapici et al. 2008). Nowland et al. (2019) suggested that this gene may play a role in adaptive differences between the tropical black-lip rock oyster populations. Many genes of solute carrier family (*SLC*) differentially expressed in hyposalinity- and temperature-stressed oysters (Ertl et al. 2019), and solute carrier family 6 member 14 (*SLC6A14*) was included in one differentiation island of the HDSC01400 scaffold.

Extension of *Haliotis discus hannai* Reference Genome Based on Linkage Information

The genome assembly of *H. discus hannai* used in this study (Nam et al. 2017) is fragmented (scaffold N50 = 211,346 bp). The reason for this is that *Haliotis* species have the largest sequenced genomes among gastropods (~1.9 Gb in *H. discus hannai*), making it impossible to infer genome-wide distribution of the detected differentiation islands. More contiguous genome assemblies of *H. rufescens* (scaffold N50 = 1,895,871 bp) and *H. rubra* (scaffold N50 = 1,227,833 bp) have been obtained using the Chicago method and Nanopore sequencing (Gan et al. 2019; Masonbrink et al. 2019). Nevertheless, chromosome-level genome assemblies of *Haliotis* have not been available. To overcome this limitation, we increased the contiguity of *H. discus hannai* genome using linkage information from a full-sib family bred in captivity. This family has been used for linkage map construction with microsatellite DNA markers (Sekino and Hara 2007b). The parents and 96 full-sibs were genotyped for 175,768 SNP loci across the genome using the GRAS-Di method, and these SNP loci were used for scaffolding with SELDLA, which extend scaffolds based on linkage maps generated with low-depth sequencing data (Yoshitake et al. 2018). We determined locations of 4,345 scaffolds and orientations of 1,149 scaffolds out of 80,105 scaffolds, representing 54.3% and 24.7% of the *H. discus hannai* genome sequences, respectively. This extension led to 21-fold increase in N50 (scaffold N50 = 4,499,196 bp). The extended scaffolds were further anchored onto 18 linkage groups (LGs; Sekino and Hara 2007b) and assembled using the linkage maps with 167 microsatellite DNA markers (Sekino and Hara 2007b) with ALLMAPS (Tang et al. 2015). High collinearity (Pearson correlation coefficient > 0.9) of the locations of microsatellite DNA markers was indicated in 12 LGs, but not in six LGs (LG04, 11, 12, 14, 15, and 16; supplementary fig. 4, Supplementary Material online). Moreover, dot plots comparing the 18 LGs with 26 *H. rufescens* and 8 *H. rubra* scaffolds larger than 5 Mb indicated successful alignment of LG01, LG05, and LG11 (supplementary figs. 5 and 6, Supplementary Material online). Although there are still

limitations in the quality of the extended genome, we were able to map 10 of the 27 differentiation islands into LG01, LG02, LG04, LG07, LG11, LG13, LG16, and LG17 of the extended *H. discus hannai* genome (table 1). Furthermore, we observed high interchromosomal LD among divergent SNP loci/selected outliers in *H. madaka* in Sado (supplementary fig. 7, Supplementary Material online), which can be suggestive of positive selection maintaining functional associations among distant loci.

Discussion

Speciation with Gene Flow Model Fits the Western Pacific Abalones

Our population genomic analyses revealed that the sympatric Western Pacific abalones are genetically distinct even though they are capable of hybridization with high fertility (Koike et al. 1988; Ahmed et al. 2008). We found no nonsynonymous substitutions in the *Lysin* and *VERL* genes between the most closely related *H. discus* and *H. madaka* (supplementary table 1, Supplementary Material online). For *H. gigantea* that diverged from a common ancestor of *H. discus* and *H. madaka*, several nonsynonymous substitutions were identified in the *Lysin* gene but not in the *VERL* gene. These findings suggest that the coevolution of fertilization proteins is not the main factor for the nearly complete reproductive isolation of the Western Pacific abalones in the wild. On the other hand, each of the three abalone species occupies different depth zones (fig. 1A). A previous study suggested that fertilization rates of abalones decrease when the physical distance between males and females is about 2 m or more during spawning (Babcock and Keesing 1999). Also, although geographical distributions of *H. discus* and *H. madaka* overlap, Sakai and Shimamoto (1978) reported slight differences in the microgeographical distribution of these species. Therefore, it seems likely that reproductive isolation of the Western Pacific abalones is caused by ecological factors, such as habitat separation.

Although the three species are genetically distinct and reciprocally monophyletic, ABBA–BABA analyses suggested historical hybridization among all three species. This inference was backed up by results of demographic modeling, suggesting that the speciation of these taxa could have occurred in the face of gene flow (cf., Nosil 2012). Given the extensive sharing of mitogenome haplotypes between *H. discus discus* and *H. madaka*, as well as clear signs of introgression from *H. discus discus* to *H. madaka* in one *H. madaka* population shown by clustering analyses and demographic modeling, the reproductive isolation between the sympatric *H. discus discus* and *H. madaka* is still developing in the face of spatially varying interspecies gene flow. Also, lack of shared mitogenome haplotypes and admixture in the clustering analyses suggest that recent hybridization has not occurred, or has rarely occurred, between *H. gigantea* and *H. discus discus*/*H. madaka*, but demographic modelling results indicated that hybridization between these species has occurred during their speciation processes, suggesting speciation-with-gene flow in the Western Pacific abalones. Our demographic modeling also suggested secondary contact in both speciation events, suggesting

that initial allopatric or reduced gene flow phase is important for speciation in the free-spawning marine invertebrates. This implies that marine invertebrate speciation consists of allopatric and sympatric phases, which conforms to traditional ideas in ecological speciation (Rundle and Nosil 2005).

Past phylogenetic analyses suggested close genetic relationships between the Western Pacific and North American abalones (Lee and Vacquier 1995; Streit et al. 2006), and North American abalones are considered to have more derived morphological characters than the Western Pacific abalones (Geiger and Groves 1999). Based on this, the Western Pacific abalones are considered to have diverged from the amphi-Pacific abalones, which radiated in California during glacial cycles (Geiger and Groves 1999). This hypothesis is in line with the result of our phylogenomic analyses. Although it is difficult to estimate the divergence times among the Western Pacific abalones because information on the mutation rates of marine invertebrates is limited, our demographic modeling using the human mutation rate (2.5×10^{-8}; Nachman and Crowell 2000) suggests that *H. gigantea* diverged 14 million years ago (Ma) and *H. discus* and *H. madaka* diverged 3 Ma assuming generation time of 3 years (*H. discus* in the wild reach sexual maturity as 3- or 4-year-olds; Yu et al. 2018). Fossil records of *H. discus* and *H. gigantea* in Pliocene have been reported (Geiger and Groves 1999). It is notable that 14 Ma is the time when the Sea of Japan opened by the rotation of the Japanese archipelago (Chinzei 1986) and that 3 Ma corresponds to the time after which the Sea of Japan was repeatedly closed (Tada 1994). These paleogeographic isolation events of the Sea of Japan have led to several allopatric divergences in coastal species (Kojima et al. 1997, 2004; Akihito et al. 2008; Kokita and Nohara 2011; Hirase et al. 2012; Hirase and Ikeda 2014). Therefore, speciation of Western Pacific abalones in Japanese archipelago might have started before the Pleistocene due to these complex paleogeographic events (Kitamura et al. 2001; Kitamura and Kimoto 2006), and interspecific gene flow has continued until now.

It is noteworthy that relatively more nonsynonymous substitutions than synonymous substitutions in the *Lysin* gene were detected only in *H. gigantea* that diverged first. This means that the evolution of *Lysin* and *VERL* begins after long-term ecological separation of *H. gigantea*, and which is consistent with the assumption that allopatry is the essence of coevolution of gamete recognition (Palumbi 2009). This coevolution was hypothesized to be induced by sexual conflict resulting from polyspermy (Clark et al. 2009), and polyspermy is more likely to occur in high population density. One common ecological situation in which population densities might increase is when a species invades a new habitat (Palumbi 2009). Therefore, we can speculate that long-term ecological separation and increase of population density of *H. gigantea* led to sperm competition and evolution of *Lysin* gene with selective sweep as suggested by Clark et al. (2009). Alternatively, given that continued gene flow between *H. gigantea* and other two species, reinforcement driven

by hybrid disadvantage may also be involved in the *Lysin* evolution (Palumbi 2009). In any case, the absence of any mutations in *VERL* suggests that the evolution of fertilization genes after ecological separation is ongoing in *H. gigantea*.

Differentiation Islands of the Western Pacific Abalones

Under a secondary contact scenario fitting to the Western Pacific abalones, genomic differentiation first builds up over time due to genetic drift during a period of geographical isolation. After secondary contact, gene flow between populations gradually erodes differentiation outside barrier loci and regions with increased background selection (Cruickshank and Hahn 2014; Burri 2017; Ravinet et al. 2017). Whether differentiation becomes erased in most genomic regions or only in a few depends on the level of gene flow and the duration of allopatric isolation. The low-level differentiation between *H. discus* and *H. madaka* (fig. 4) appears to fit to the former scenario with the 27 differentiation islands representing possible barrier loci. Previous studies suggest that loci causing speciation with gene flow are likely to be located in relatively few linked clusters within the genome (Feder et al. 2012; Cruickshank and Hahn 2014). Extension of the reference genome of *H. discus hannai* based on linkage information made it possible to investigate the genomic locations of the 27 differentiation islands, and to discover that the candidate genomic regions were located at least in eight different LGs. Therefore, our data suggest that genomic regions responsible for abalone speciation are distributed in multiple chromosomes, even if the species are at early stages of speciation continuum.

A key prediction of speciation with gene flow model is that causal loci of speciation should have both high relative divergence (F_{ST}) and absolute divergence (d_{XY}; Cruickshank and Hahn 2014). However, d_{XY} values of most of the differentiation islands between most closely related *H. discus* and *H. madaka* were not high in comparison to other regions. Background selection has been identified as a mechanism generating such pattern of differentiation (Cruickshank and Hahn 2014; Burri 2017). However, background selection is not likely to explain this differentiation pattern because high F_{ST} and low d_{XY} were specific for the pair of most closely related *H. discus* and *H. madaka*. Contrary to the d_{XY}, the d_A between *H. discus* and *H. madaka* was relatively high in the differentiation islands. The likely explanation for relatively low d_{XY} in the differentiation islands is recent ecological selection, which reduces *pi* in *H. discus* and *H. madaka*, whereas continued gene flow in the genomic background can likely explain the relatively high *pi* for these two species. These findings are consistent with a simulation study of Cruickshank and Hahn (2014) showing that there is a difference in the power of F_{ST} and d_{XY} in identifying barrier loci contributing to recent divergences in the presence of high gene flow. On the other hand, the differentiation islands showed high d_{XY} as well as F_{ST} and d_A values between *H. discus* and *H. gigantea*, as well as between *H. madaka* and *H. gigantea*, suggesting that the low

background *pi* in *H. gigantea* is due to long-term isolation (cf., fig. 5C).

The *H. madaka* population in Sado with enhanced genomic introgression from *H. discus* showed high observed heterozygosity in 23 divergence and 30 outlier loci within the 27 differentiation islands. In particular, genomic introgression in the differentiation islands around 23 divergence loci seems robust because these loci were fixed for different alleles in each of *H. discus* and *H. madaka*. Simultaneously, this population showed high interchromosomal LD, which supports the hypothesis that these genomic regions are associated with reductions in hybrid survival and reproductive isolation (Bradbury et al. 2014). These findings suggest that the differentiation islands are indeed associated with the ecological divergence between *H. discus* and *H. madaka*, but have not worked as stable barrier loci between the two species (cf., Han et al. 2017); temporal and/or spatial weakening of the ecologically based divergent selection has facilitated gene flow and prevented accumulation of fixed differences. Available evidence suggests that fluctuating selective pressures are a widespread phenomenon (e.g., Nosil 2012). All this said, the observed high F_{ST}, d_{XY}, and d_A characterizing differentiation between *H. gigantea* and *H. discus* or *H. madaka* suggest that the differentiation islands are likely to work as barrier loci on longer time scales.

In conclusion, our findings suggest that the Western Pacific abalones, *H. discus*, *H. madaka*, and *H gigantea*, are going through speciation-with-gene flow under ecological separation, which was initiated in allopatry. Speciation in the abalones has proceeded to different stages in different species pairs: Barriers to gene flow are incomplete among the younger divergence of *H. discus* and *H. madaka* but fairly complete in the case of older divergences of *H. gigantea* and other two species in which evolution of fertilization proteins has taken place. Hence, the Western Pacific abalones provide insight into the genomic processes taking place in the early phase of speciation continuum before coevolution of interacting fertilization proteins has started.

Materials and Methods

Samples
From 2000 to 2008, we collected abalone individuals from 15 sampling locations along the coastline of Japan (fig. 1B; supplementary table 5, Supplementary Material online). These samples were provided by local fishermen, and species identification was conducted by us. *Hatiois discus* is classified into two subspecies, *H. discus hannai* and *H. discus discus* on the basis of sampling locations (Ino 1952; see fig. 1A for their geographic distributions). This is because these two subspecies show only slight morphological difference in dorsal surface of the shell (Ino 1952), and hence, are difficult to distinguish based on morphological features. Therefore, we assigned *H. discus* populations into *H. discus hannai*, *H. discus discus*, and into boundary populations based on the geographic location of the sampling sites (Ino 1952). Tissue samples of the Red abalones (*H. rufescens*) from California were used as outgroups. For all species, DNA was extracted from

foot muscles using the phenol/chloroform method with TNES-urea buffer (Asahida et al. 1996) or Gentra Puregene Tissue Kit (QIAGEN) and stored at $-30\,°C$ before analyses.

Mitogenome Sequencing and Analyses
Primer sets for PCR used for mitochondrial DNA sequencing were designed for 15 genes, including *COI*, *COII*, *COIII*, *ND1*, *ND2*, *ND3*, *ND4*, *ND4L*, *ND5*, *ND6*, *ATP6*, *ATP8*, *Cyt b*, *12SrRNA*, and *16SrRNA* (supplementary table 6, Supplementary Material online). PCR mixture (26 µl) contained 50 ng of template DNA, 2.5 µl of 10× Blend Taq-Plus- Buffer, 0.25 µl of Blend Taq-Plus-polymerase (0.65 units) (Toyobo), 2.5 µl of dNTPs Mixture (2 mM), and 1 µl of each primer (50 µM). Thermal cycling in PCR consisted of initial denaturation at $94\,°C$ for 2 min, followed by 35 cycles of $94\,°C$ for 30 s, $53\,°C$ for 30 s, and $72\,°C$ for 1 min. The PCR products were purified with AMPure XP Kit (Beckman Coulter) and were bidirectionally sequenced with the BigDye Terminator v3.1 Cycle Sequencing Kit (Thermo Fisher Scientific) in combination with an ABI 3730 capillary sequencer (Thermo Fisher Scientific) using the forward and reverse primers used for PCR.

Sequences were aligned using ClustalW in the MEGA 5 with default parameters. DNAcollapser of FaBox (Villesen 2007) was used to assign individuals to respective haplotypes. Obtained haplotype sequences were deposited to the EMBL/DDBJ/GenBank database. The length of the concatenated sequences (13 protein and 2 rRNA-coding genes) was trimmed to 7,837 base pairs due to the poor quality of sequences in some individuals. Neighbor-joining tree (Saitou and Nei 1987) was constructed in MEGA 5 (Tamura et al. 2011) using the Jukes–Cantor distance measure (Jukes and Cantor 1969), with an option of 95%-cutoff partial deletion. The statistical credibility of the resulting tree was evaluated with 1,000 bootstrap replications. We note that the Jukes–Cantor distance performs well in estimating phylogenetic relationships among closely related lineages (Nei and Kumar 2000; Hirase et al. 2016). Genetic differentiation among species was assessed by AMOVA (Excoffier et al. 1992) using Arlequin ver. 3.5 (Excoffier et al. 2005).

GRAS-Di Sequencing
The GRAS-Di method, which was developed by Toyota Motor Corp. (Enoki and Takeuchi 2018), was used for genome-wide DNA sequencing. The patent for GRAS-Di is currently available under the license agreement or contract-based analysis services. This method generates a sequence library consisting of amplicons created by two rounds of PCR using random primers and sequence adapter sequences. The final PCR product is purified using either columns or magnetic beads without size selection, and then sequenced on an Illumina platform. This simple method allowed us to obtain the genotypes at several thousands of loci across the genome. Details of this method are given in Hosoya et al. (2019). All library constructions and sequencing were carried out at Eurofins Japan. The GRAS-Di reads were filtered by Trimmomatic ver. 0.38 (-*phred33 ILLUMINACLIP TruSeq3-SE.fa:2:40:15 LEADING:10 TRAILING:10 SLIDINGWINDOW:4:20 MINLEN:32*) to remove Illumina adapters and low-quality

regions. The filtered reads were aligned to the *H. discus hannai* genome sequence (Nam et al. 2017) using the BWA-MEM algorithm in BWA ver. 0.7.8 (Li and Durbin 2009) with default settings, followed by local realignment around indels by GATK ver. 3.7 (McKenna et al. 2010) with default settings. After these alignment procedures, multimapped reads (indicated by "XA" and "SA" tags in their BAM records) were removed. Mapping statistics are shown in supplementary table 7, Supplementary Material online. SNPs were called using SAMtools ver. 1.9 mpileup and bcftools and filtered using VCFtools ver. 0.1.12 (−minQ 20 −remove-indels −maf 0.05 −max-alleles 2 −min-meanDP 15 −minDP 10) (Danecek et al. 2011). The MAF filtering option was omitted when we generated a vcf file for demographic modeling. To remove potential genotyping errors (e.g., due to allele dropout), SNP loci were removed if the proportion of missing genotypes was >10% at least in one of five genetic groups (*H. discus hannai*, boundary populations of *H. discus hannai* and *H. discus discus*, *H. discus discus*, *H. madaka*, and *H. gigantea*) that were pruned using pop_missing_filter.sh of dDocent ver. 2.2.7 package (Puritz et al. 2014). Finally, SNP loci that showed departure from the Hardy–Weinberg equilibrium (*P* < 0.001) in all genetic groups were removed using the script filter_hwe_by_pop.pl of the dDocent package. (Of note, no SNP locus was filtered with this criterion.)

Whole-Genome Sequencing
Genome sequencing was performed for the four abalone species (supplementary table 8, Supplementary Material online) using Illumina HiSeq X Ten with the 250-bp paired-end protocol. All library construction and sequencing were carried out at BGI, China. The paired-end reads were filtered by Trimmomatic to remove the adapter, Illumina-specific sequences and low-quality regions (-phred33 ILLUMINACLIP TruSeq3-SE.fa:2:40:15 LEADING:10 TRAILING:10 SLIDINGWINDOW:4:20 MINLEN:32). The filtered paired-end reads were aligned to the *H. discus hannai* genome sequence (Nam et al. 2017) using the BWA-MEM algorithm in BWA with default settings, followed by local realignment around indels by GATK ver. 3.7 with default settings. Multimapped reads were removed in the same manner as described above. Mapping statistics are shown in supplementary table 8, Supplementary Material online. SNPs were called using SAMtools mpileup (-Q 30) and bcftools, and filtered using VCFtools (−minQ 20 −remove-indels −maf 0.05 −max-alleles 2 −minDP 6 -max-missing-count 1).

Gene Prediction and Annotation of *H. discus hannai* genome
We downloaded RNA sequencing data for *H. discus hannai* individuals from the NCBI Sequence Read Archive (SRA, Leinonen et al. 2011): SRR1910554, SRR1943392, SRR1944101, SRR1944137, SRR1985199, SRR1985200, SRR1985201, SRR1987402, SRR1987403, SRR1987404, SRR2057965, SRR2057966, SRR2057969, SRR2058004, SRR2058005, SRR2058006, SRR2059857, SRR2059863, SRR2059864, SRR2059865, SRR5082552, SRR5082554, SRR5082555, SRR5083065, SRR5083066, SRR5083067, SRR6459616, SRR6459617, SRR6459618, SRR6459619,

SRR7956997, SRR7956998, SRR7956999, SRR7957000, SRR7957001, SRR7957002, SRR7967467, SRR7967468, and SRR7967469. All RNA sequencing reads were aligned to the *H. discus hannai* genome sequence as single-end reads using HISAT2 ver. 2.1.0 (Kim et al. 2019). Stringtie ver. 1.3.5 (Pertea et al. 2015) was used to predict transcript structures based on the aligned reads. Third, we identified candidate coding regions within transcript sequences using TransDecoder ver. 5.5.0 (https://github.com/TransDecoder/TransDecoder, last accessed July 14, 2021). These analyses were performed with default set tings. An annotation file is available from Dryad (https://doi.org/10.5061/dryad.gf1vhhmq5).

Gene functions were annotated using BlastP searches (*E*-value cut-off: e-10) against the *nr* database of NCBI.

Phylogenomic Analyses of the Western Pacific and North American Abalones
To infer genetic relationships among the Western Pacific and North American abalones, we constructed a phylogenomic tree using our whole-genome sequencing data of the Western Pacific abalones and North American abalones. Whole-genome sequencing data of North American abalones, except for *H. rufescens*, were downloaded from the NCBI SRA (SRR7958743−SRR7958752; Masonbrink et al. 2019). The paired-end reads were filtered and aligned to the *H. discus hannai* genome sequence in the same manner as described above. SNPs were called using SAMtools mpileup (-Q 30) and bcftools and filtered using VCFtools (−minDP 10 −remove-indels −max-missing-count 0). A maximum likelihood (ML) tree was constructed using RAxML ver. 8.2.12 (Stamatakis 2014) with 1,000 bootstrap replicates using the GTRGAMMA model of nucleotide substitution with a correction for ascertainment bias (-m ASC_GTRGAMMA −asc-corr=stamatakis -f a -# 1000) (Leaché et al. 2015). Invariant sites were removed using *ascbias.py* (https://github.com/btmartin721/raxml_ascbias, last accessed July 14, 2021).

Population Genomics Analyses Based on GRAS-Di Data
Genetic diversity (observed heterozygosity) of each abalone species and population was estimated using GenoDive ver. 2.0b27 (Meirmans and Van Tienderen et al. 2004). LD between SNP loci was evaluated based on r^2 values calculated using PLINK ver. 1.07 (Purcell et al. 2007). Site-F_{ST} values were calculated using VCFtools and those in monomorphic sites and under zero were converted to zero. To infer the genetic relationships among the Western Pacific abalones, we constructed an ML tree using RAxML as mentioned above. A clustering analysis was performed using ADMIXTURE (Alexander et al. 2009) assuming *K* from 1 to 10 with default parameters . To alleviate the effect of LD on the clustering analysis, we retained one SNP locus every 5,000 bp using "−thin 5,000" command in vcftools. Cross-validation scores were used to determine the most appropriate *K* (Alexander and Lange 2011). We analyzed genotypes of the Sado population of *H. madaka* using NewHybrids ver. 1.1. This analysis was performed using the genotypes of *H. discus* and *H.*

madaka (except for the Sado population) as parental genotypes with 10,000 burnin iterations, and 50,000 iterations.

We used four outlier tests to search for signatures of selection between *H. discus* and *H. madaka*: BayeScan (Foll and Gaggiotti 2008), *pcadapt* (Luu et al. 2017), FLK (Bonhomme et al. 2010), and the coalescent method of Beaumont and Nichols (1996) as implemented in Arlequin (referred to as the Fdist method). For BayeScan analyses, we set prior odds to 10 to minimize chances of false positives and ran 5,000 pilot runs, followed by 100,000 iterations (5,000 samples, a thinning interval of 10, and a burn-in of 50,000) ($FDR < 0.05$). For *pcadapt* analyses, SNP loci that significantly contributed to the first principal component separating *H. discus* and *H. madaka* were retrieved ($FDR < 0.01$). For the Fdist analyses, we used the island model with 100 simulated demes and 20,000 coalescent simulations ($P < 0.05$). FLK analyses were performed with default settings ($P < 0.05$). Outliers identified consistently in all tests were considered as putative loci under selection. To annotate and predict the effects of SNPs, we used SnpEff (Cingolani et al. 2012) based on a custom database using a gff3 file of *H. discus hannai* genome.

Evolutionary history of Western Pacific abalone speciation process was investigated with ML-based demographic inference based on SFS using the program fastsimcoal2. The folded three-population multidimensional observed SFS from GRAS-Di SNP data was obtained with easySFS.py (https://github.com/isaacovercast/easySFS, last accessed July 14, 2021). As sample sizes varied among populations, we narrowed down to 30 chromosomes per population (i.e., 15 diploid individuals) to project the SFS. Five models of divergence were tested (fig. 3A), and for all them, priors were drawn from a uniform log distribution. Because there are no estimates of nuclear mutation rates for abalones, we applied a rate of 2.5×10^{-8} in humans (Nachman and Crowell 2000). For each model, we performed 100 independent runs of 100,000 coalescent simulations to obtain ML estimates of model parameters. Model selection was performed using the run with the highest likelihood for each of the models. Following Meier et al. (2017), AIC was used for model selection and assessing the likelihood distribution for each model by calculating the likelihoods of 100 SFS derived from 1,000,000 coalescent simulations. We derived 95% confidence intervals for parameter estimates from the models using nonparametric site bootstrapping where we resampled SNP loci with replacement. We created 100 bootstrapped SFSs and then performed ten independent runs of likelihood estimation on them. Estimates from each of the best runs were then used to derive the 95% confidence intervals around all parameter estimates from the focal model. Details of each model are available from Dryad (https://doi.org/10.5061/dryad.gf1vhhmq5).

Population Genomics Analyses Based on Whole-Genome Sequencing Data

Genome-wide genetic diversity and differentiation between abalones were investigated by calculating *pi*, F_{ST}, and d_{XY} values for nonoverlapping 20-kb sliding windows using a python script of Martin et al. (2013) (https://github.com/simonhmartin/genomics_general, last accessed July 14,

2021). d_A was calculated as $d_{XY} - (pi_X + pi_Y)/2$. To test for gene flow among abalones, we performed the ABBA–BABA test using popstats (*D* statistics were calculated as (BABA − ABBA)/(BABA + ABBA); Skoglund et al. 2015). A *z*-score with an absolute value of 3 or more was considered to be evidence of significant gene flow (Reich et al. 2009; Green et al. 2010). A test for interspecies gene flow based on f_d-statistics, a modified version of ABBA–BABA statistics, in nonoverlapping 20-kb sliding windows was also performed using the python script of Martin et al. (2015).

Elongation of *H. discus hannai* scaffolds

To increase the contiguity of *H. discus hannai* genome (Nam et al. 2017), we used linkage information from one captive bred full-sib family of this species (family "F") used earlier for microsatellite DNA-based linkage map construction (Sekino and Hara 2007b). The parents and their 96 full-sib offspring were genotyped for SNPs obtained with the GRAS-Di method; the obtained SNP loci were scaffolded with SELDLA ver. 2.0.9 (Yoshitake et al. 2018). The minimum depth in SNP filtering (DP) was set to 5, and the extended scaffolds were anchored into 18 LGs (36 diploid chromosomes) containing 167 microsatellite DNA markers (Sekino and Hara 2007b) with ALLMAPS (Tang et al. 2015). The genomic position of each microsatellite marker in the SELDLA-extended *H. discus hannai* reference genome was determined by the BlastN search. Dot plots used to explore homology were generated using minimap2 (Li 2018). Minimap2 results were converted to tab-delimited text using a portable pipeline software (https://github.com/c2997108/OpenPortable Pipeline, last accessed July 14, 2021), and regions with continuous alignment of at least 1,000 bp were retained.

Supplementary Material

Supplementary data are available at *Molecular Biology and Evolution* online.

Acknowledgments

Author Contributions

S.H., M.S., and K.K. designed the study. M.S. and M.H. provided tissue and DNA samples. S.H., M.N., M.I., and M.S. performed wet laboratory experiments and collected data. S.H. and Y.Y. performed genome analyses. S.H., J.M., and K.K. wrote the manuscript with the help of Y.Y., M.S., M.I., and M.H. All authors approved the final version of the manuscript.

Data Availability

All mitochondrial sequence data are available from DDBJ under accession numbers: LC613253–LC616030; the DDBJ accession numbers of the data of the whole-genome sequencing (DRR276780–DRR276816), GRAS-Di sequencing (DRR276817–DRR277014). Other data for analysis are available on Dryad (https://doi.org/10.5061/dryad.gf1vhhmq5).

References

Ahmed F, Koike Y, Strüssmann CA, Yamasaki I, Yokota M, Watanabe S. 2008. Genetic characterization and gonad development of artificially produced interspecific hybrids of the abalones, *Haliotis discus discus* Reeve, *Haliotis gigantea* Gmelin and *Haliotis madaka* Habe. *Aquac Res.* 39(5):532–541.

Akihito, Fumihito A, Ikeda Y, Aizawa M, Makino T, Umehara Y, Kai Y, Nishimoto Y, Hasegawa M, Nakabo T, et al. 2008. Evolution of Pacific Ocean and the Sea of Japan populations of the gobiid species, *Pterogobius elapoides* and *Pterogobius zonoleucus*, based on molecular and morphological analyses. *Gene* 427(1–2):7–18.

Alexander DH, Lange K. 2011. Enhancements to the ADMIXTURE algorithm for individual ancestry estimation. *BMC Bioinformatics* 12(1):246.

Alexander DH, Novembre J, Lange K. 2009. Fast model-based estimation of ancestry in unrelated individuals. *Genome Res.* 19(9):1655–1664.

An H-S, Jee Y-J, Min K-S, Kim B-L, Han S-J. 2005. Phylogenetic analysis of six species of Pacific abalone (Haliotidae) based on DNA sequences of 16s rRNA and cytochrome c oxidase subunit I mitochondrial genes. *Mar Biotechnol (NY).* 7(4):373–380.

Anderson E, Thompson E. 2002. A model-based method for identifying species hybrids using multilocus genetic data. *Genetics* 160(3):1217–1229.

Asahida T, Kobayashi T, Saitoh K, Nakayama I. 1996. Tissue preservation and total DNA extraction from fish stored at ambient temperature using buffers containing high concentration of urea. *Fish Sci.* 62(5):727–730.

Babcock R, Keesing J. 1999. Fertilization biology of the abalone *Haliotis laevigata*: laboratory and field studies. *Can J Fish Aquat Sci.* 56(9):1668–1678.

Beaumont MA, Nichols RA. 1996. Evaluating loci for use in the genetic analysis of population structure. *Proc R Soc Lond B Biol Sci.* 263(1377):1619–1626.

Begun DJ, Holloway AK, Stevens K, Hillier LW, Poh Y-P, Hahn MW, Nista PM, Jones CD, Kern AD, Dewey CN, et al. 2007. Population genomics: whole-genome analysis of polymorphism and divergence in *Drosophila simulans*. *PLoS Biol.* 5(11):e310.

Bester-van der Merwe AE, D'Amato ME, Swart BL, Roodt-Wilding R. 2012. Molecular phylogeny of South African abalone, its origin and evolution as revealed by two genes. *Mar Biol Res.* 8(8):727–736.

Bierne N, Bonhomme F, David P. 2003. Habitat preference and the marine-speciation paradox. *Proc R Soc Lond B Biol B.* 270(1522):1399–1406.

Bonhomme M, Chevalet C, Servin B, Boitard S, Abdallah J, Blott S, SanCristobal M. 2010. Detecting selection in population trees: the Lewontin and Krakauer test extended. *Genetics* 186(1):241–262.

Bradbury IR, Bowman S, Borza T, Snelgrove PV, Hutchings JA, Berg PR, Rodríguez-Ezpeleta N, Lighten J, Ruzzante DE, Taggart C. 2014. Long distance linkage disequilibrium and limited hybridization suggest cryptic speciation in Atlantic cod. *PLoS One* 9:e106380.

Burri R. 2017. Interpreting differentiation landscapes in the light of long-term linked selection. *Evol Lett.* 1(3):118–131.

Chinzei K. 1986. Opening of the Japan Sea and marine biogeography during the Miocene. *J Geomagn Geoelec.* 38(5):487–494.

Cingolani P, Platts A, Wang LL, Coon M, Nguyen T, Wang L, Land SJ, Lu X, Ruden DM. 2012. A program for annotating and predicting the effects of single nucleotide polymorphisms, SnpEff: SNPs in the genome of *Drosophila melanogaster* strain w1118; iso-2; iso-3. *Fly (Austin)* 6(2):80–92.

Clark NL, Gasper J, Sekino M, Springer SA, Aquadro CF, Swanson WJ. 2009. Coevolution of interacting fertilization proteins. *PLoS Genet.* 5(7):e1000570.

Cruickshank TE, Hahn MW. 2014. Reanalysis suggests that genomic islands of speciation are due to reduced diversity, not reduced gene flow. *Mol Ecol.* 23(13):3133–3157.

Danecek P, Auton A, Abecasis G, Albers CA, Banks E, DePristo MA, Handsaker RE, Lunter G, Marth GT, Sherry ST, et al.; 1000 Genomes Project Analysis Group. 2011. The variant call format and VCFtools. *Bioinformatics* 27(15):2156–2158.

De Wit P, Palumbi SR. 2013. Transcriptome-wide polymorphisms of red abalone (*Haliotis rufescens*) reveal patterns of gene flow and local adaptation. *Mol Ecol.* 22(11):2884

Enoki, H, Takeuchi, Y, editors. 2018. New genotyping technology, GRAS-Di, using next generation sequencer. Proceedings of the Plant and Animal Genome Conference XXVI. San Diego, CA. Available from: https://pag.confex.com/pag/xxvi/meetingapp.cgi/Paper/29067.

Ertl NG, O'Connor WA, Elizur A. 2019. Molecular effects of a variable environment on Sydney rock oysters, *Saccostrea glomerata*: thermal and low salinity stress, and their synergistic effect. *Mar Genomics.* 43:19–32.

Excoffier L, Dupanloup I, Huerta-Sánchez E, Sousa VC, Foll M. 2013. Robust demographic inference from genomic and SNP data. *PLoS Genet.* 9(10):e1003905.

Excoffier L, Laval G, Schneider S. 2005. Arlequin (version 3.0): an integrated software package for population genetics data analysis. *Evol Bioinform Online.* 1:117693430500100–117693430500150.

Excoffier L, Smouse PE, Quattro JM. 1992. Analysis of molecular variance inferred from metric distances among DNA haplotypes: application to human mitochondrial DNA restriction data. *Genetics* 131(2):479–491.

Feder JL, Egan SP, Nosil P. 2012. The genomics of speciation-with-gene-flow. *Trends Genet.* 28(7):342–350.

Foll M, Gaggiotti O. 2008. A genome-scan method to identify selected loci appropriate for both dominant and codominant markers: a Bayesian perspective. *Genetics* 180(2):977–993.

Galindo BE, Vacquier VD, Swanson WJ. 2003. Positive selection in the egg receptor for abalone sperm lysin. *Proc Natl Acad Sci U S A.* 100(8):4639–4643.

Gan HM, Tan MH, Austin CM, Sherman C, Wong YT, Strugnell J, Gervis M, McPherson L, Miller A. 2019. Best foot forward: nanopore long reads, hybrid meta-assembly and haplotig purging optimises the first genome assembly for the Southern Hemisphere blacklip abalone (*Haliotis rubra*). *Front Genet.* 10:889.

Geiger DL, Groves LT. 1999. Review of fossil abalone (Gastropoda: Vetigastropoda: Haliotidae) with comparison to recent species. *J Paleontol.* 73(5):872–885.

Green RE, Krause J, Briggs AW, Maricic T, Stenzel U, Kircher M, Patterson N, Li H, Zhai W, Fritz MH-Y, et al. 2010. A draft sequence of the Neandertal genome. *Science* 328(5979):710–722.

Han F, Lamichhaney S, Grant BR, Grant PR, Andersson L, Webster MT. 2017. Gene flow, ancient polymorphism, and ecological adaptation shape the genomic landscape of divergence among Darwin's finches. *Genome Res.* 27(6):1004–1015.

Hara M, Fujio Y. 1992. Geographic distribution of isozyme genes in natural abalone. *Bull Tohoku Natl Fish Res Inst.* 54:115–124.

Hara M, Sekino M. 2005. Genetic difference between Ezo-awabi *Haliotis discus hannai* and Kuro-awabi *H. discus discus* populations: microsatellite-based population analysis in Japanese abalone. *Fish Sci.* 71(4):754–766.

Hirase S, Ikeda M. 2014. Divergence of mitochondrial DNA lineage of the rocky intertidal goby *Chaenogobius gulosus* around the Japanese Archipelago: reference to multiple Pleistocene isolation events in the Sea of Japan. *Mar Biol.* 161(3):565–574.

Hirase S, Ikeda M, Kanno M, Kijima A. 2012. Phylogeography of the intertidal goby *Chaenogobius annularis* associated with paleoenvironmental changes around the Japanese Archipelago. *Mar Ecol Prog Ser.* 450:167–179.

Hirase S, Takeshima H, Nishida M, Iwasaki W. 2016. Parallel mitogenome sequencing alleviates random rooting effect in phylogeography. *Genome Biol Evol.* 8(4):1267–1278.

Hosoya S, Hirase S, Kikuchi K, Nanjo K, Nakamura Y, Kohno H, Sano M. 2019. Random PCR-based genotyping by sequencing technology GRAS-Di (genotyping by random amplicon sequencing, direct) reveals genetic structure of mangrove fishes. *Mol Ecol Resour.* 19(5):1153–1163.

Ino T. 1952. Biological study on the propagation of Japanese abalone (genus *Haliotis*). *Bull Tokai Reg Fish Res Lab.* 5:1–102.

Itami K, Takeda R, Sakai T, Shimamoto N. 1978. Distribution and growth of the young abalone, *Nordotis gigantea* (GMELIN), from south coast of Awaji Island in Hyogo Prefecture. *Bull Hyogo Pref Fish Exp Stn.* 18:15–28.

Jones MR, Mills LS, Alves PC, Callahan CM, Alves JM, Lafferty DJ, Jiggins FM, Jensen JD, Melo-Ferreira J, Good JM. 2018. Adaptive introgression underlies polymorphic seasonal camouflage in snowshoe hares. *Science* 360(6395):1355–1358.

Jukes TH, Cantor CR. 1969. Evolution of protein molecules. In: Munro RE, editor. Mammalian protein metabolism. New York: Academic Press, pp. 21–132.

Kim D, Paggi JM, Park C, Bennett C, Salzberg SL. 2019. Graph-based genome alignment and genotyping with HISAT2 and HISAT-genotype. *Nat Biotechnol.* 37(8):907–915.

Kitamura A, Kimoto K. 2006. History of the inflow of the warm Tsushima Current into the Sea of Japan between 3.5 and 0.8 Ma. *Palaeogeogr Palaeoclimatol Palaeoecol.* 236(3–4):355–366.

Kitamura A, Takano O, Takata H, Omote H. 2001. Late Pliocene-early Pleistocene paleoceanographic evolution of the Sea of Japan. *Palaeogeogr Palaeoclimatol Palaeoecol.* 172(1–2):81–98.

Koike Y, Sun Z-X, Takashima F. 1988. On the feeding and growth of juvenile hybrid abalones. *Aquac Sci.* 36(3):231–235.

Kojima S, Hayashi I, Kim D, Iijima A, Furota T. 2004. Phylogeography of an intertidal direct-developing gastropod *Batillaria cumingi* around the Japanese Islands. *Mar Ecol Prog Ser.* 276:161–172.

Kojima S, Segawa R, Hayashi I. 1997. Genetic differentiation among populations of the Japanese turban shell *Turbo* (*Batillus*) *cornutus* corresponding to warm currents. *Mar Ecol Prog Ser.* 150:149–155.

Kokita T, Nohara K. 2011. Phylogeography and historical demography of the anadromous fish *Leucopsarion petersii* in relation to geological history and oceanography around the Japanese Archipelago. *Mol Ecol.* 20(1):143–164.

Leaché AD, Banbury BL, Felsenstein J, De Oca AN-M, Stamatakis A. 2015. Short tree, long tree, right tree, wrong tree: new acquisition bias corrections for inferring SNP phylogenies. *Syst Biol.* 64(6):1032–1047.

Lee Y-H, Vacquier V. 1995. Evolution and systematics in Haliotidae (Mollusca: Gastropoda): inferences from DNA sequences of sperm lysin. *Mar Biol.* 124(2):267–278.

Leinonen R, Sugawara H, Shumway M, International Nucleotide Sequence Database Collaboration. 2011. The sequence read archive. *Nucleic Acids Res.* 39(Database issue):D19–D21.

Lessios HA. 2007. Reproductive isolation between species of sea urchins. *Bull Mar Sci.* 81(2):191–208.

Li H. 2018. Minimap2: pairwise alignment for nucleotide sequences. *Bioinformatics* 34(18):3094–3100.

Li H, Durbin R. 2009. Fast and accurate short read alignment with Burrows–Wheeler transform. *Bioinformatics* 25(14):1754–1760.

Luu K, Bazin E, Blum MG. 2017. pcadapt: an R package to perform genome scans for selection based on principal component analysis. *Mol Ecol Resour.* 17(1):67–77.

Martin SH, Dasmahapatra KK, Nadeau NJ, Salazar C, Walters JR, Simpson F, Blaxter M, Manica A, Mallet J, Jiggins CD. 2013. Genome-wide evidence for speciation with gene flow in *Heliconius* butterflies. *Genome Res.* 23(11):1817–1828.

Martin SH, Davey JW, Jiggins CD. 2015. Evaluating the use of ABBA–BABA statistics to locate introgressed loci. *Mol Biol Evol.* 32(1):244–257.

Masonbrink RE, Purcell CM, Boles SE, Whitehead A, Hyde JR, Seetharam AS, Severin AJ. 2019. An annotated genome for *Haliotis rufescens*

(red abalone) and resequenced green, pink, pinto, black, and white abalone species. *Genome Biol Evol.* 11(2):431–438.

McKenna A, Hanna M, Banks E, Sivachenko A, Cibulskis K, Kernytsky A, Garimella K, Altshuler D, Gabriel S, Daly M, et al. 2010. The Genome Analysis Toolkit: a MapReduce framework for analyzing next-generation DNA sequencing data. *Genome Res.* 20(9):1297–1303.

Meier JI, Sousa VC, Marques DA, Selz OM, Wagner CE, Excoffier L, Seehausen O. 2017. Demographic modelling with whole-genome data reveals parallel origin of similar *Pundamilia* cichlid species after hybridization. *Mol Ecol.* 26(1):123–141.

Meirmans PG, Van Tienderen PH. 2004. GENOTYPE and GENODIVE: two programs for the analysis of genetic diversity of asexual organisms. *Mol Ecol Notes.* 4(4):792–794.

Miglietta MP, Faucci A, Santini F. 2011. Speciation in the sea: overview of the symposium and discussion of future directions. *Integr Comp Biol.* 51(3):449–455.

Momigliano P, Jokinen H, Fraimout A, Florin A-B, Norkko A, Merilä J. 2017. Extraordinarily rapid speciation in a marine fish. *Proc Natl Acad Sci U S A.* 114(23):6074–6079.

Nachman MW, Crowell SL. 2000. Estimate of the mutation rate per nucleotide in humans. *Genetics* 156(1):297–304.

Nam B-H, Kim H, Seol D, Kim H, Noh ES, Kim EM, Noh JK, Kim Y-O, Park JY, Kwak W. 2021. Genotyping-by-Sequencing of the regional Pacific abalone (*Haliotis discus*) genomes reveals population structures and patterns of gene flow. *PLoS One* 16(4):e0247815.

Nam B-H, Kwak W, Kim Y-O, Kim D-G, Kong HJ, Kim W-J, Kang J-H, Park JY, An CM, Moon J-Y, et al. 2017. Genome sequence of pacific abalone (*Haliotis discus hannai*): the first draft genome in family Haliotidae. *Gigascience* 6(5):1–8.

Nei M, Kumar S. 2000. Molecular evolution and phylogenetics. Oxford: Oxford University Press.

Nei M, Li W-H. 1979. Mathematical model for studying genetic variation in terms of restriction endonucleases. *Proc Natl Acad Sci U S A.* 76(10):5269–5273.

Nosil P. 2012. Ecological speciation. Oxford: Oxford University Press.

Nowland SJ, Silva CN, Southgate PC, Strugnell JM. 2019. Mitochondrial and nuclear genetic analyses of the tropical black-lip rock oyster (*Saccostrea echinata*) reveals population subdivision and informs sustainable aquaculture development. *BMC Genomics* 20(1):711.

Oziolor EM, Reid NM, Yair S, Lee KM, VerPloeg SG, Bruns PC, Shaw JR, Whitehead A, Matson CW. 2019. Adaptive introgression enables evolutionary rescue from extreme environmental pollution. *Science* 364(6439):455–457.

Palumbi S. 2009. Speciation and the evolution of gamete recognition genes: pattern and process. *Heredity (Edinb)* 102(1):66–76.

Palumbi SR. 1992. Marine speciation on a small planet. *Trends Ecol Evol.* 7(4):114–118.

Pertea M, Pertea GM, Antonescu CM, Chang T-C, Mendell JT, Salzberg SL. 2015. StringTie enables improved reconstruction of a transcriptome from RNA-seq reads. *Nat Biotechnol.* 33(3):290–295.

Pogson GH. 2016. Studying the genetic basis of speciation in high gene flow marine invertebrates. *Curr Zool.* 62(6):643–653.

Puebla O. 2009. Ecological speciation in marine vs. freshwater fishes. *J Fish Biol.* 75(5):960–996.

Purcell S, Neale B, Todd-Brown K, Thomas L, Ferreira MAR, Bender D, Maller J, Sklar P, de Bakker PIW, Daly MJ, et al. 2007. PLINK: a tool set for whole-genome association and population-based linkage analyses. *Am J Hum Genet.* 81(3):559–575.

Puritz JB, Hollenbeck CM, Gold JR. 2014. dDocent: a RADseq, variant-calling pipeline designed for population genomics of non-model organisms. *PeerJ.* 2:e431.

Puritz JB, Keever CC, Addison JA, Byrne M, Hart MW, Grosberg RK, Toonen RJ. 2012. Extraordinarily rapid life-history divergence between *Cryptasterina* sea star species. *Proc R Soc Lond B Biol Sci.* 279(1744):3914–3922.

Ravinet M, Faria R, Butlin R, Galindo J, Bierne N, Rafajlović M, Noor M, Mehlig B, Westram A. 2017. Interpreting the genomic landscape of

speciation: a road map for finding barriers to gene flow. *J Evol Biol.* 30(8):1450–1477.

Reich D, Thangaraj K, Patterson N, Price AL, Singh L. 2009. Reconstructing Indian population history. *Nature* 461(7263):489–494.

Rhode C, Vervalle J, Bester-van der Merwe AE, Roodt-Wilding R. 2013. Detection of molecular signatures of selection at microsatellite loci in the South African abalone (*Haliotis midae*) using a population genomic approach. *Mar Genomics.* 10:27–36.

Rundle HD, Nosil P. 2005. Ecological speciation. *Ecol Lett.* 8(3):336–352.

Saitou N, Nei M. 1987. The neighbor-joining method: a new method for reconstructing phylogenetic trees. *Mol Biol Evol.* 4(4):406–425.

Sakai T, Shimamoto N. 1978. Distribution of abalones from the coastal waters of Awaji Island in Hyogo Prefecture. *Bull Hyogo Pref Fish Exp Stn.* 18:11–14.

Seehausen O, Butlin RK, Keller I, Wagner CE, Boughman JW, Hohenlohe PA, Peichel CL, Saetre G-P, Bank C, Brännström A, et al. 2014. Genomics and the origin of species. *Nat Rev Genet.* 15(3):176–192.

Sekino M, Hara M. 2007a. Individual assignment tests proved genetic boundaries in a species complex of Pacific abalone (genus *Haliotis*). *Conserv Genet.* 8(4):823–841.

Sekino M, Hara M. 2007b. Linkage maps for the Pacific abalone (genus *Haliotis*) based on microsatellite DNA markers. *Genetics* 175(2):945–958.

Skoglund P, Mallick S, Bortolini MC, Chennagiri N, Hünemeier T, Petzl-Erler ML, Salzano FM, Patterson N, Reich D. 2015. Genetic evidence for two founding populations of the Americas. *Nature* 525(7567):104–108.

Stamatakis A. 2014. RAxML version 8: a tool for phylogenetic analysis and post-analysis of large phylogenies. *Bioinformatics* 30:1312–1313.

Streit K, Geiger DL, Lieb B. 2006. Molecular phylogeny and the geographic origin of Haliotidae traced by haemocyanin sequences. *J Molluscan Stud.* 72(1):105–110.

Tada R. 1994. Paleoceanographic evolution of the Japan Sea. *Palaeogeogr Palaeoclimatol Palaeoecol.* 108(3–4):487–508.

Tamura K, Peterson D, Peterson N, Stecher G, Nei M, Kumar S. 2011. MEGA5: molecular evolutionary genetics analysis using maximum likelihood, evolutionary distance, and maximum parsimony methods. *Mol Biol Evol.* 28(10):2731–2739.

Tang H, Zhang X, Miao C, Zhang J, Ming R, Schnable JC, Schnable PS, Lyons E, Lu J. 2015. ALLMAPS: robust scaffold ordering based on multiple maps. *Genome Biol.* 16(1):3.

Van Doorn GS, Luttikhuizen PC, Weissing FJ. 2001. Sexual selection at the protein level drives the extraordinary divergence of sex–related genes during sympatric speciation. *Proc R Soc Lond B Biol B.* 268(1481):2155–2161.

Villesen P. 2007. FaBox: an online toolbox for fasta sequences. *Mol Ecol Notes.* 7(6):965–968.

Wang X, Wang S, Li C, Chen K, Qin JG, Chen L, Li E. 2015. Molecular pathway and gene responses of the pacific white shrimp *Litopenaeus vannamei* to acute low salinity stress. *J Shellfish Res.* 34(3):1037–1048.

Wu CI. 2001. The genic view of the process of speciation. *J Evol Biol.* 14(6):851–865.

Yapici N, Kim Y-J, Ribeiro C, Dickson BJ. 2008. A receptor that mediates the post-mating switch in Drosophila reproductive behaviour. *Nature* 451(7174):33–37.

Yoshitake K, Igarashi Y, Mizukoshi M, Kinoshita S, Mitsuyama S, Suzuki Y, Saito K, Watabe S, Asakawa S. 2018. Artificially designed hybrids facilitate efficient generation of high-resolution linkage maps. *Sci Rep.* 8(1):1–10.

Yu L, Xu D, Ye H, Yue H, Ooka S, Kondo H, Yazawa R, Takeuchi Y. 2018. Gonadal transcriptome analysis of pacific abalone *Haliotis discus discus*: identification of genes involved in germ cell development. *Mar Biotechnol (NY).* 20(4):467–480.